Experimental and numerical analyses of angle bracket connections in cross laminated timber structures

by

S. Saeed Rezvani

A Thesis Submitted in Partial Fulfillment
of the Requirements for the Degree of

MASTER OF APPLIED SCIENCE

in the Department of Civil Engineering

University of Victoria

We acknowledge with respect the Lekwungen peoples on whose traditional territory the university stands and the Songhees, Esquimalt and W̱SÁNEĆ peoples whose historical relationships with the land continue to this day.

Experimental and numerical analyses of angle bracket connections in cross laminated timber structures

By

S. Saeed Rezvani
MASc., University of Victoria, 2021

Supervisory Committee

Dr. Lina Zhou, Supervisor
Department of Civil Engineering

Dr. Chun Ni, Outside Member
Advanced Building Systems, FPInnovations

Abstract

The invention of mass timber products, including cross laminated timber (CLT), over the past two decades has made tall wood building possible. In CLT structures, angle brackets are commonly used in wall-to-floor connections to transfer the shear in seismic and wind loads. In reality, these connections could experience loads in various directions, as well as multi-directional forces. This research consists of two parts: an experimental study carried out in Part 1, followed by a numerical program completed in Part 2. The research aims to investigate the performance of wall-to-floor CLT angle bracket connections under various loading situations.

In Part 1 of the research, a two-phase experimental program consisting of 12 monotonic tests in the first phase, and 24 monotonic and 24 cyclic tests in the second phase was conducted to investigate the behaviour of wall-to-floor CLT angle bracket connections. Connections were assembled using two different sizes of steel angle brackets and four types of fasteners, under uplift, in-plane shear, and out-of-plane shear loads. The performance of the connections was evaluated in terms of strength, stiffness, ductility, energy dissipation capacity, and failure modes. Results show that small diameter fasteners are more desirable for wood-to-wood angle bracket connections in terms of failure modes, load-bearing capacity and stiffness. Specimens exhibited considerable ductile performance under both uplift and in-plane shear loads due to combinations of yielding of brackets and yielding or pull-out of screws. Connections loaded under out-of-plane tension may fail in the splitting of CLT panels. Fully-threaded screws led to higher strength, stiffness and energy dissipation capacity but less ductility compared to partially-threaded screws in angle bracket connections.

In Part 2 of the research, a two-phase numerical program was carried out to assess the coupling effect of biaxial loading on the performance of CLT wall-to-floor angle bracket connections. In Phase I, a 3D finite element model of connections was developed using ABAQUS software and verified with the data from experimental tests carried out in Part 1 of the research. In Phase II of the numerical program, the verified model was used to simulate the performance of connections under three biaxial loads, i.e., shear and in-plane uplift, shear and out-of-plane tension, and shear and out-of-plane compression. The coupling effect on the performance of the connections was evaluated in terms of strength, stiffness, ductility, and failure modes under biaxial loads, and compared with the scenario where the connection was only loaded in shear. Results show that the

application of biaxial loading may considerably decrease the shear performance of the connections. Additionally, the results confirm the analytical equation suggested by the European Technical Assessment to predict the resistance of angle bracket connections under biaxial loads.

Table of Contents

List of Figures

List of Tables

Author Contributions

The core of this thesis is composed of two chapters. The contents presented in Chapter 2 have been published [2] and the contents described in Chapter 3 have been submitted. The author list, title, and author contributions are clarified below for each core chapter.

[2] S. Rezvani, L. Zhou, and C. Ni, “Experimental evaluation of angle bracket connections in CLT structures under in- and out-of-plane lateral loading”.

Saeed Rezvani: Investigation, Methodology, Formal analysis, Writing - original draft

Lina Zhou: Conceptualization, Methodology, Funding acquisition, Supervision, Resources, Writing - review & editing

Chun Ni: Conceptualization, Methodology, Writing - review & editing

[3] S. Rezvani, L. Zhou, and C. Ni, “Numerical analysis of in- and out-of-plane coupling effects on angle bracket connections in CLT structures”.

Saeed Rezvani: Investigation, Methodology, Modelling and simulation, Formal analysis, Writing - original draft

Lina Zhou: Conceptualization, Methodology, Funding acquisition, Supervision, Resources, Writing - review & editing

Chun Ni: Conceptualization, Methodology, Writing - review & editing

Acknowledgments

The completion of this thesis would not have been possible without the unconditional love and unlimited support of my partner, Moloud, and my family throughout this journey.

I would like to acknowledge the support and patience of my supervisor, Dr. Lina Zhou, and co-supervisor, Dr. Chun Ni, whose guidance was invaluable in the completion of this project. I would also like to thank MTC Solutions Inc. for their support.

Additionally, I would like to thank my research group at the University of Victoria who put up with my never-ending questions and created many memorable moments.

Dedication

In dedication to

All the students who lost their lives aboard Flight PS752,

&

All the Indigenous children who have suffered years of injustice and discrimination, and to the children who didn't come home from residential school.

May their memories forever stay with us.

Chapter 1: Introduction

Over the last few decades, timber structures have continuously increased their footprint in the construction industry [1]–[3]. Timber construction is environmentally sustainable and the manufacturing process of wood products emits significantly less carbon compared to classical structural materials (e.g. steel and concrete). Additionally, the easy assembly process and rapid erection at the construction site make timber construction financially and operationally favourable. The inherent lightness of wood and its high strength-to-weight ratio make such structures particularly suitable for their use in seismically active regions [1]–[8]. However, the orthotropic properties of wood (i.e. different material properties in different directions) result in more complex failure mechanisms compared to isotropic materials (e.g. steel) [9]. The development of Engineered Wood Products (EWP) and the emergence of mass timber structures in the late 1990s and early 21st century have improved the limitations of timber as a construction material and boosted high-rise timber construction [1], [10]. The Province of British Columbia passed the Wood First Act [11] in 2009 to promote the use of wood in construction by requiring provincially-funded projects to use wood as the primary construction material. Consequently, several Canadian provinces applied changes to their building codes allowing light-frame wood buildings to rise to six stories. In 2019, British Columbia adjusted its building code to allow up to 12-storey mass timber buildings, and the National Building Code of Canada followed suit in 2020. Additionally, in the United States, International Code Council approved a set of proposals in 2019 allowing up to 18 stories of Type IV-A (i.e. non-combustible) mass timber construction for Business and Residential Occupancies as a part of the 2021 International Building Code [6], [12]–[15]. These legislative changes along with the technical advancements in the timber construction industry have created new possibilities for utilizing wood in construction.

Cross Laminated Timber (CLT) is a quasi-rigid composite plate-like EWP, commonly composed of an uneven number (usually three, five or seven layers) of crosswise glued-laminated panels. Relatively high stiffness, dimensional stability, and in- and out-of-plane load-bearing capacity of CLT make CLT an attractive construction material for wall and floor elements in timber or hybrid structures [1], [2], [6], [10], [16], [17]. The adhesive bond used in CLT panels toughens them against splitting and mitigates the problems associated with traditional timber products [3]. The acoustic, thermal, and fire-resistant properties are also enhanced in CLT panels [8]. Although

being much lighter, the mechanical properties of CLT panels are similar to those of normal-weight RC slabs of equal thickness [3]. This lightness makes it possible to minimize required materials in foundations and superstructures, and thus makes it an ideal material in regions with high seismic risks [3], [7], [8]. Despite their recent introduction, CLT structures have rapidly spread globally. Voll Arkitekter's Mjøstårne (Brumunddal, Norway) and Brock Commons (Vancouver, Canada) with 85 and 53m in height, respectively, are among the tallest mass timber buildings at this time [18]–[21].

Connections are arguably the most critical part of timber structures [22]. Connections provide continuity to the system and control the behaviour of the structures by transferring forces between different elements of the structure, anchoring the superstructure to the foundation, and maintaining the integrity of the system [1], [2], [22], [23]. Ottenhaus et al. [24] argue that structures should be capable of resisting horizontal loads (i.e. wind, seismic, etc.) as well as vertical gravity loads. Horizontal loads apply a certain amount of energy to the system that should be somehow dissipated. According to Pozza et al. [25], energy dissipation in structural systems may happen through different mechanisms. Low-intensity actions may fully rely on frictional effects and structural viscous damping of timber elements to dissipate the energy, with the connection remaining in the elastic range with no or minimal contribution to the energy dissipation process. In mid- and high-intensity cases, on the other hand, a different mechanism activates. While CLT panels have high stiffness and strength properties compared to metal connectors [26], [27], they cannot dissipate mid- and high-intensity energy during an earthquake due to their inherently brittle behaviour in bending and tension [4]. According to Jorissen and Fragiacomo [28], structures should be designed to fail in ductile manners to provide sufficient warning to the occupants before a failure happens, allow stress redistribution in statically indeterminate structures, allow energy dissipation under seismic loading, and increase structural robustness. Hence, it is crucial to utilize mechanical connections to ensure a ductile failure mode and avoid brittle failure mechanisms. Also, D'Arenzo et al. [4] mention that, unlike light-timber frame structures where the energy dissipation happens largely in the wall elements at the sheathing-to-framing connections, metal connectors play the key role in the energy dissipation in CLT structures.

The connections must be able to control the static and cyclic behaviour of CLT structures by exhibiting high levels of ductility and absorbing large amounts of energy to lower the wind- and

earthquake-induced loads applied to the systems [4], [29], [30]. Even with the existence of metal connectors, the systems can exhibit brittle failures (e.g. ruptures in the metal connection plates or welded joints, pull-out of the base anchor, etc.) if they are not designed properly according to capacity design and over-strength principles [4], [5], [24], [25], [27], [28]. To avoid brittle failures and to ensure robustness and ductility against lateral loads, a strength hierarchy should be defined with some certain members assigned as weak links to dissipate energy and provide system ductility [24]. Often in timber structures, metal connectors are the so-called weak links that undergo plastic deformation to dissipate the energy while other members are designed to remain in the elastic range. Concurrently, the connections must maintain adequate strength and stiffness to resist lateral and axial forces without undergoing excessive deformations [6], [9], [30]–[33].

Steel angle brackets, hold-downs, and self-tapping screws are the most common connectors in mass timber structures [12]. Many researchers have studied the performance of CLT connections in various loading scenarios [2], [4], [36], [5], [12], [20], [25], [27], [30], [34], [35]. Gavric et al. [27] studied the performance of angle bracket and hold-down connections under shear and uplift loadings, respectively. Tomasi and Smith [3] assessed the performance of several steel angle brackets in shear via monotonic and cyclic tests and compared the results to simplified analytical methods. Liu and Lam [37] investigated the impact of uplift deformation on the shear performance of angle bracket connections. Through experimental tests, they applied monotonic and cyclic shear displacements to the connections, with four levels of constant uplift forces being applied simultaneously. D'Arenzo et al. [4] used monotonic tests and numerical analyses to evaluate the mechanical properties of an innovative metal angle bracket connection in uplift and shear directions. Pozza et al. [25] used the results of their monotonic and cyclic tests to validate their numerical model and, and then used the model to analyze the coupled behaviour of angle bracket connections under simultaneous uplift and shear forces. Some studies have suggested a simplified approach to designing CLT structures by suggesting that hold-downs and angle brackets work solely in uplift and shear, respectively [21], [38]. For example, D'Arenzo et al. [38] claim that uniformly-spaced angle brackets mainly work to transfer the shear force between walls and floors and prevent sliding mechanism under wind or seismic load, while hold-downs work only in uplift to control the rocking behaviour of the system. Other studies, however, have acknowledged the contribution of angle brackets in resisting uplift forces [20], [27], [34]. Gavric et al. [27] reported that angle brackets exhibited significant strength and stiffness in both shear and uplift directions.

Similar results were also found by Flatscher et al. [39] and Casagrande et al. [34] for different types of angle brackets.

Since angle bracket connections are a vital part of mass timber structures, this two-part research aimed to develop a wholesome understanding of their performance under various loading scenarios. Each part of this study was motivated by an existing knowledge gap. The following briefly elaborates on the problem addressed in each part, and the methods used.

Part 1 (2): Although many researchers have studied the performance of CLT angle bracket connections under in-plane (parallel to wall plane) shear and uplift loads, no research was found that explores the performance of these connections under out-of-plane (perpendicular to wall plane) loads. In reality, however, these connections need to transfer out-of-plane forces, induced by wind and earthquakes, between wall and floor panels. To bridge this gap, a series of monotonic and cyclic tests were designed and carried out to explore the capacity of angle bracket connections in four directions (two in-plane and two out-of-plane). The results are presented in terms of strength, stiffness, ductility, energy dissipation, and failure modes in each direction.

Part 2 (3): The second part of this research was concerned with the bi-axial performance of CLT angle bracket connections. Similar to Part 1, although a few researchers have studied the coupled in-plane shear-uplift performance of these connections [4], [30], [33], [37], there was a lack of research on the impact of out-of-plane forces on the in-plane shear performance of angle bracket connections. To fill this gap, a 3D finite element ABAQUS model was developed and verified using test data from Part 1. The verified model was then used to simulate the performance of angle bracket connections under a variety of biaxial loads, some of which included out-of-plane tension and compression loads. Contrary to the majority of numerical studies that use two-node non-linear spring elements to simulate the behaviour of fasteners in connections, this model relies solely on 3D elements for all parts, including fasteners, and considered the physical interactions between the fasteners and other parts. This approach provides better insight into the potential failure mechanisms of angle bracket connections in biaxial loading scenarios.

The last chapter of this thesis (**4**) discusses key findings and recommendations of this research.

This thesis follows the manuscript-based format. 2 and 3 represent two manuscripts. The contents presented in 2 have been published [2] and the contents described in 3 have been submitted. Since

the ‘Introduction’ sections of Chapters 2-3 include literature reviews, a separate literature review chapter is not included to avoid repetition.

Chapter 2: Experimental evaluation of angle bracket connections in CLT structures under in- and out-of-plane lateral loading

2.1 Introduction

Since its invention, cross laminated timber (CLT) has been extensively used as an alternative to concrete and steel in medium- and high-rise buildings due to its environmental sustainability, rapidity of construction, high dimensional stability and excellent fire performance [1], [3], [4], [6]. In Canada, the 2020 National Building Code (NBC) allows up to 12-storey mass timber construction [15]. In the US, the 2021 International Building Code (IBC) allows up to 18 stories of non-combustible mass timber construction for business and residential occupancies [14].

Steel angle brackets, hold-downs, and self-tapping screws are the most commonly used connectors in CLT structures [1], [3], [4], [6], [21]. Since connections control the behaviour and maintain the integrity of CLT structures [1], [22], [23], a good understanding of them through experimental tests is necessary to predict the performance of CLT structures [24]. Experimental results are also critical for the development and verification of numerical studies [17]. Many researchers have studied the behaviour of CLT connections [1], [3], [35], [37]–[39], [4], [8], [20], [21], [25], [27], [30], [34]. Gavric et al. [27] tested the performance of angle brackets and hold-downs in shear and uplift directions, respectively, under monotonic and cyclic loads. Tomasi and Smith [3] carried out monotonic and fully-reversed cyclic tests to assess the performance of several steel angle brackets in shear and compared the results to simplified analytical methods. Liu and Lam [37] completed an experimental campaign to investigate the effect of uplift deformation on the shear behaviour of angle bracket connections. They tested the connections under monotonic and cyclic shear loadings, with four levels of constant uplift forces being applied simultaneously. D'Arenzo et al. [4] used monotonic tests and finite element analyses to evaluate the mechanical properties of an innovative metal angle bracket connection in uplift and shear directions. Pozza et al. [25] developed a coupled uplift-shear finite-element model and validated the model with the results of monotonic and cyclic tests to analyze the coupled behaviour of angle bracket connections under simultaneous application of uplift and shear forces. For the function of angle brackets and hold-downs to resist the in-plane lateral load, some studies have suggested a simplified approach

to design CLT structures by considering that hold-downs and angle brackets work solely in uplift and shear, respectively [21], [38]. D'Arenzo et al. [38], for example, claims that hold-downs work in uplift and control the rocking behaviour of the system, while angle brackets largely work to transfer the shear force and prevent sliding mechanism under wind or seismic load. Other studies, however, acknowledge the contribution of angle brackets in resisting uplift forces [1], [20], [27], [34]. Gavric et al. [27] reported that angle brackets exhibited significant strength and stiffness in both shear and uplift directions. Similar results were also found by Flatscher et al. [39] and Casagrande et al. [34] for different types of angle brackets.

Although extensive research has been done on the behaviour of CLT angle bracket connections under uplift and in-plane shear loads, no study was found on the performance of such connections under out-of-plane (perpendicular to wall plane) loads. In reality, these connections also need to be designed to transfer perpendicular to wall forces induced by wind and earthquakes to its adjacent floors or roofs. A two-phase experimental study was carried out to assess the capacity of angle bracket connections in four directions (two in-plane and two out-of-plane). The most efficient fastener type for angle bracket connections was determined in Phase I and used in Phase II to investigate the performance of the connections under different load directions. The results are presented in terms of strength, stiffness, ductility, energy dissipation, and failure modes in each direction.

2.2 Materials

Two types of angle brackets (BB A90 and A105) were used in this study (**Figure 2.1** a). Both brackets are one-piece hot-rolled angle brackets, reinforced with an embossed rib, and used for wood-to-wood or wood-to-concrete connections. The brackets are made of pre-galvanized steel with a thickness of 1.5 mm and punched with 5 and 13 mm holes [40]. A90 brackets (90 × 65 mm flange) have symmetric hole arrangement with one big and 10 small holes on each flange, while A105 brackets (105 × 90 mm flange) have an asymmetric setting with 10 small and 3 big holes on one flange, and 16 small and one big hole on the other flange (**Figure 2.1** a) [40]. 3-ply (35 mm/ply) SPF (Spruce-Pine-Fir) CLT panels were used in the tests. All panels had been stored in a controlled environment with a temperature of 20°C and relative humidity of 65% for at least three weeks before assembling and testing. The major direction of the wall panel is always vertical

(perpendicular to the wall-floor intersection line), while the major direction of the floor panel can be parallel or perpendicular to the wall-floor intersection line. In this project, the major direction of the floor panel is set to be parallel to the wall-floor intersection line to differ it from the wall panel (**Figure 2.1** b). In the A105 bracket, the flange with three big holes is always connected to the floor panel, and the other flange is connected to the wall panel. Four types of fasteners were used in this study, as shown from left to right in **Figure 2.1** (c): ASSY 12.7 × 80 mm screw, partially-threaded ASSY 4.5 × 50 mm screw, fully-threaded 4.5 × 50 mm screw, and threaded 4.5 × 50 mm ring nail.

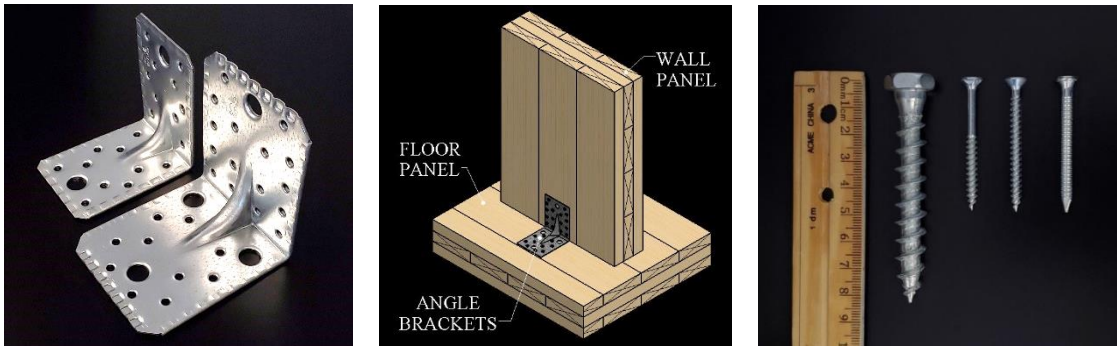

(a) (b) (c)

Figure 2.1. Angle brackets and fasteners in a CLT connection (a) A90 (farther) and A105 (closer) angle brackets, (b) CLT floor and wall panels' configuration, and (c) fasteners.

2.3 Phase I

The objective of Phase I research was to find the most efficient fastener type investigated in this project. 12 monotonic tests were carried out in Phase I with A105 angle brackets in uplift (F1 in **Figure 2.2**) and in-plane shear (F2 in **Figure 2.2**) directions (**Table 2.1**). F1 and F2 tests aimed to assess the resistance of connections against rocking and sliding behaviours of the wall, respectively. F3 and F4 loads will be applied to specimens in Phase II to assess the out-of-plane shear performance of angle bracket connections.

Table 2.1. Test plans and fastener details for Phase I tests.

Loading Type and Direction	Angle Bracket Type	Fastener Type	Fastener count (per bracket) and bearing forces		No. of Tests	Total No. of Tests
			Connected to floor	Connected to wall		
Monotonic Uplift (F1)	A105	4.5 mm nails	10 (withdrawal)	16 (shear)	2	12
		4.5 mm screws	10 (withdrawal)	16 (shear)	2	
		12.7 mm screws	3 (withdrawal)	1 (shear)	2	
Monotonic Shear (F2)	A105	4.5 mm nails	10 (shear)	16 (shear)	2	
		4.5 mm screws	10 (shear)	16 (shear)	2	
		12.7 mm screws	3 (shear)	1 (shear)	2	

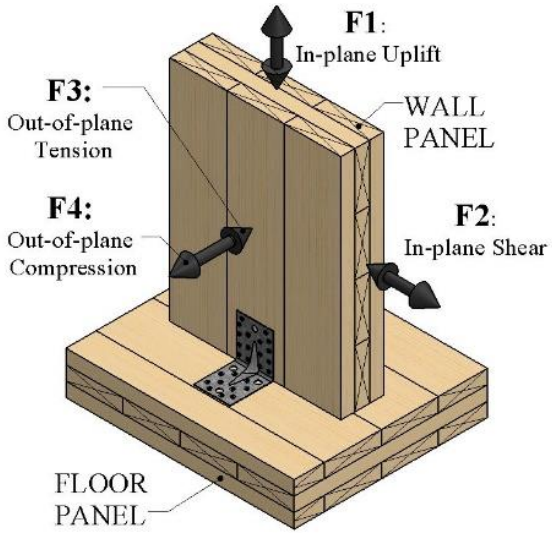

Figure 2.2. Loading directions in CLT-angle bracket tests.

2.3.1 Phase I – Test Setup

Figure 2.3 shows the monotonic uplift (F1) test configuration. A compression load was applied on the wall (middle) panel to simulate the uplift load. With this setup, although the block-shear failure at the end of the wall panel was prevented due to the extension of the wall panel beyond the floor, this failure mode was not expected in these tests since 16 fasteners connected to the wall panel (working in shear) were stronger than the 10 fasteners connected to the floor panel (working in withdrawal). **Figure 2.4** shows the in-plane shear (F2) test configuration. A compression load

was applied on the wall (middle) panel to simulate the shear force. In practice, angle bracket connections are normally placed on one side of exterior walls and on both sides of interior walls. In this project, symmetric setups were adopted for both tests to prevent rotations as suggested by ETA [40] and protect the testing machine from bending moment [41]. It should be noted that with the symmetric setup, the load-displacement response is the average response of all the angle bracket connections in a specimen. Due to the redistribution of internal forces among connections, the obtained load-displacement curves can be treated as the average performance of angle bracket connections. A displacement-controlled setting with a constant rate of 0.05 mm/s was used for both tests and the tests were continued until the load dropped below 80% of the peak load. Four Linear Variable Displacements Transducers (LVDTs) were used to measure the relative movement of panels. The average of LVDT readings was used in the result analysis.

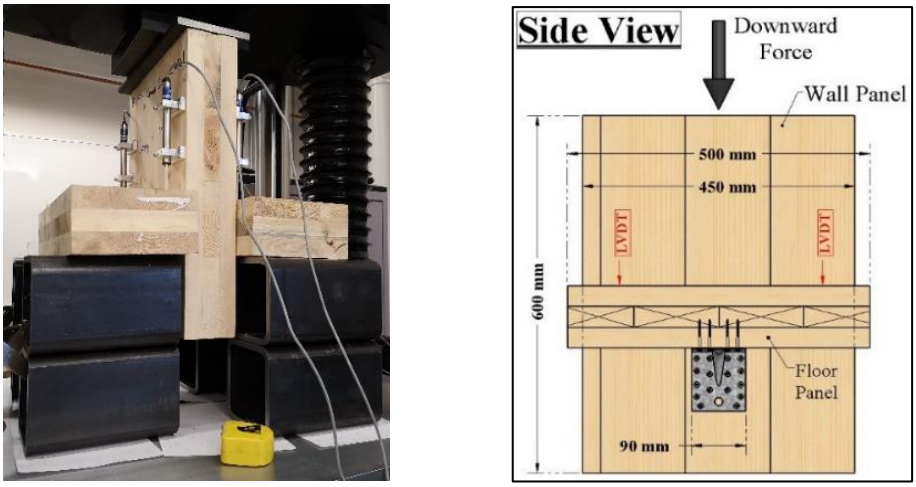

(a) (b)

Figure 2.3. Monotonic uplift (F1) test setup: (a) test photo (with fixtures) and (b) side view.

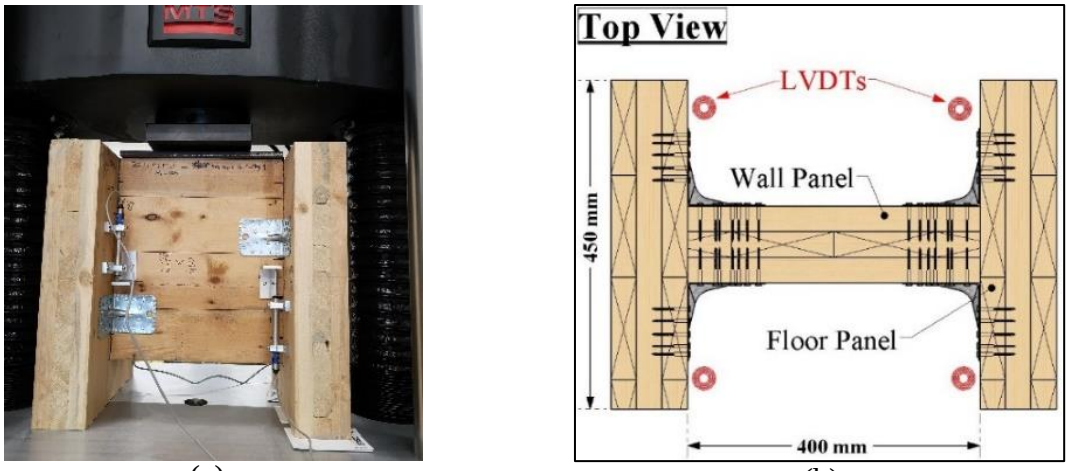

(a) (b)

Figure 2.4. Monotonic in-plane shear (F2) test setup: (a) test photo and (b) top view.

2.3.2 Phase I – Results and Discussion

Test results were evaluated following the procedure prescribed in ASTM E2126 [42]. Equivalent energy elastic-plastic (EEEP) curves were developed for each set of data to determine the mechanical properties including the yield load (P_y), displacement at yield (Δ_y), peak load (P_{peak}), displacement at peak load (Δ_{peak}), ultimate displacement (Δ_u), load at ultimate displacement (P_u), and stiffness (k). All mechanical properties and load-deformation curves were calculated for each test. Due to the limited replicates tested in this project, the average values and curves are reported and discussed for every set of tests. **Figure 2.5** shows the average load-displacement curves of Phase I monotonic uplift (F1) tests. In these tests, different diameter of fasteners led to different failure modes and stiffness but comparable load resistance. For connections with 12.7 mm screws, only one screw resisted shear on the wall flange. The hole started to expand at small forces due to stress concentration which resulted in smaller secant stiffness values (50%) compared to the other two types of connections (**Table 2.2**). The high stress concentration led to the tear-out failure of the wall flange of brackets (**Figure 2.6** a). For angle bracket connections with 4.5 mm ring nails and screws, failures happened due to the withdrawal of the fasteners on the floor flange along with a fracture in the embossed rib. Minor splitting of the floor panel was also observed (**Figure 2.6** b).

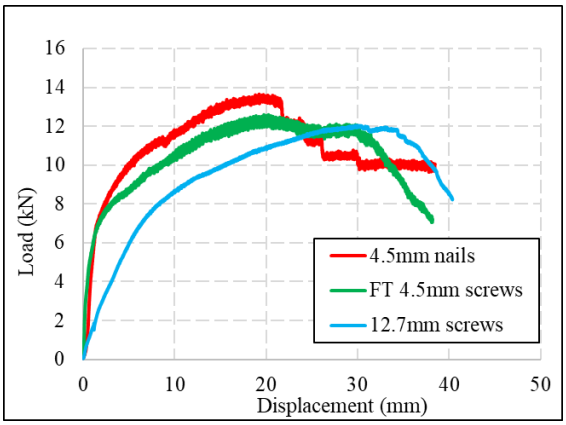

Figure 2.5. Load-displacement curves of Phase I - F1 tests (per bracket).

Table 2.2. Mechanical properties of angle bracket connections in Phase I - F1 tests.

Angle Bracket Type	Load Direction	Fastener type	Δ_y [mm]	P_y [kN]		Δ_{peak} [mm]	P_{peak} [kN]		Δ_u [mm]		P_u [kN]	K_{el} [kN/mm]	
				Mean	COV		Mean	COV	Mean	COV		Mean	COV
A105	Monotonic Uplift (F1)	4.5mm nails	3.1	11.8	0.4%	20.1	13.8	2.4%	25.7	6.3%	10.7	3.9	5.5%
		4.5mm screws	2.9	11.0	1.4%	26.0	12.7	1.2%	34.8	1.8%	10.1	3.8	2.9%
		12.7mm screws	5.6	10.5	1.1%	29.1	12.1	2.3%	37.4	1.4%	9.6	1.9	5.9%

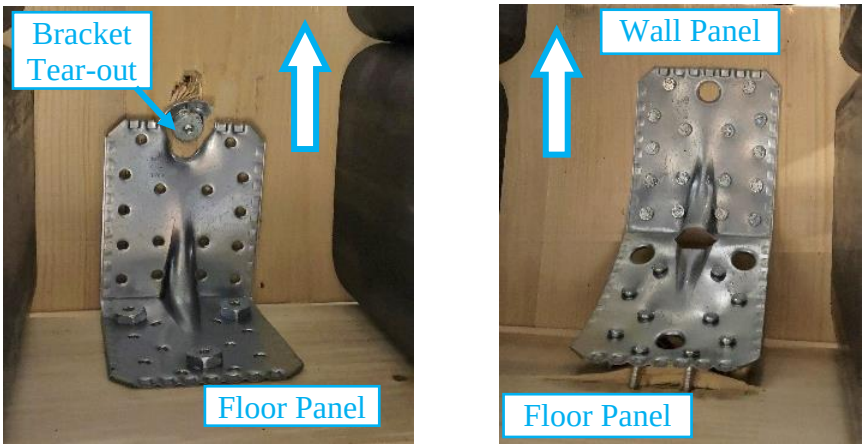

(a) (b)

Figure 2.6. Failure modes in Phase I uplift (F1) tests with (a) large screws, and (b) small nails and screws.

Figure 2.7 shows the average load-displacement curves of Phase I monotonic in-plane shear (F2) tests. In these tests, the sliding between the wall and floor panels caused angle brackets to twist. The even distribution of 4.5 mm ring nails and screws on the brackets (**Figure 2.8** a), created a higher rotational constraint in both flanges. The failures were a combination of twist and yielding of brackets and pull-out of fasteners. In large screw connection tests (**Figure 2.8** b), the flange with 3 screws was more rigidly connected to the floor panel, so the sliding was mostly accommodated by twisting and yielding of the other flange connected to the wall panel with only one screw, and eventually caused the punch-through failure in the flange attached to the floor panel. Results show that angle bracket connections with 12.7 mm screws had 55% lower resistance (P_{peak}) and 81% lower stiffness (K_{el}) than those with 4.5 mm ring nails or screws (**Table 2.3**). The low stiffness can be explained by the low capability of the single screw in restraining the rotation of the flange of the angle bracket attached to the wall panel.

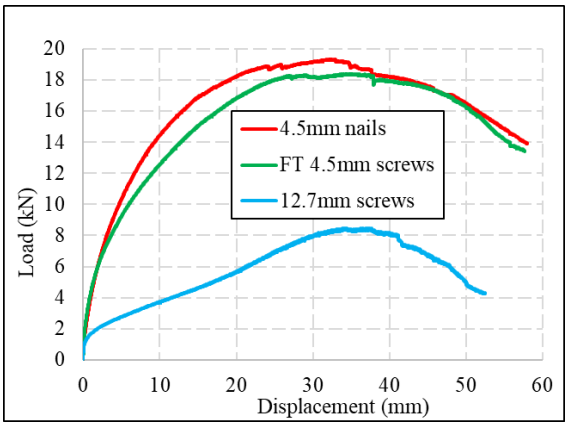

Figure 2.7. Load-displacement curves of Phase I - F2 tests (per bracket).

Table 2.3. Mechanical properties of angle bracket connections in Phase I - F2 tests.

Angle Bracket Type	Load Direction	Fastener type	Δ_y [mm]	P_y [kN]		Δ_{peak} [mm]	P_{peak} [kN]		Δ_u [mm]		P_u [kN]	K_{el} [kN/mm]	
				Mean	COV		Mean	COV	Mean	COV		Mean	COV
A105	Monotonic Uplift (F2)	4.5mm nails	6.1	17.4	7.3%	32.7	19.3	7.5%	45.7	0.3%	16.5	2.9	4.9%
		4.5mm screws	6.5	16.5	1.1%	30.3	18.7	0.4%	47.1	3.2%	16.6	2.5	2.6%
		12.7mm screws	16.2	7.3	6.4%	37.2	8.6	4.9%	43.9	4.6%	7.0	0.5	2.3%

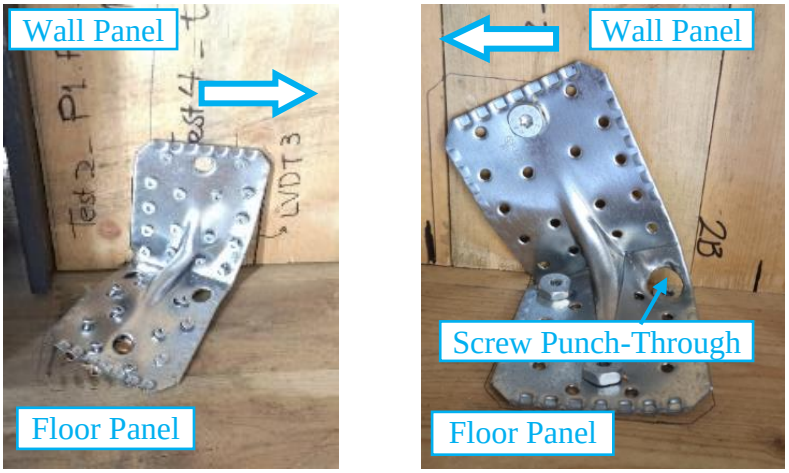

(a) (b)

Figure 2.8. Failure modes in Phase I In-plane shear tests with (a) small nails and screws, and (b) large screws.

The test results and failure modes indicate that angle bracket connections with 12.7 mm screws are not desirable. The small fasteners, however, showed very close performances concerning failure modes, load-bearing capacity and stiffness in both directions (**Table 2.3**). As a result, 4.5 mm screws were chosen for Phase II of the experimental program due to an easier assembly process compared to nails.

2.4 Phase II

To better understand the behaviour of the brackets under various loading conditions, 24 monotonic and 24 cyclic tests were carried out in Phase II, using the fastener type selected in Phase I. Two thread lengths, partially- and fully-threaded, of 4.5 mm screws were compared in this phase. In addition to F1 and F2 directions, Phase II tests considered F3 and F4 directions (see **Figure 2.2**) to evaluate the resistance of the connections against out-of-plane lateral loads. Similar to Phase I tests, Phase II monotonic tests were performed under a displacement-controlled protocol at a constant rate of 0.05 mm/s and were continued until the load dropped below 80% of the peak load. The loading protocol of cyclic tests was designed according to the ISO 16670 [43] method. The displacement amplitude increases by increments of 20% of V_u (ultimate displacement obtained in Phase I monotonic tests in each direction) until the force drops below 80% of the peak load. A displacement rate of 2 mm/s was used for all cyclic tests which lie within the range advised by the

ISO 16670 [43]. A similar data acquisition system to that of Phase I tests was used in Phase II. **Table 2.4** shows the test plans and fastener details for Phase II tests.

Table 2.4: Test plans and fastener details for Phase II tests.

Loading Type and Direction	Angle Bracket Type	Fastener Type	Fastener count (per bracket) and bearing forces		No. of Tests	Total No. of Tests
			Connected to floor	Connected to wall		
Cyclic Uplift (F1)	A90	PT 4.5 mm screw	10 (withdrawal)	10 (shear)	3	24
		FT 4.5 mm screw			3	
	A105	PT 4.5 mm screw	10 (withdrawal)	16 (shear)	3	
		FT 4.5 mm screw			3	
Cyclic Shear (F2)	A90	PT 4.5 mm screw	10 (shear)	10 (shear)	3	
		FT 4.5 mm screw			3	
	A105	PT 4.5 mm screw	10 (shear)	16 (shear)	3	
		FT 4.5 mm screw			3	
Monotonic Tension (F3)	A90	PT 4.5 mm screw	10 (shear)	10 (withdrawal)	2	24
		FT 4.5 mm screw			4	
	A105	PT 4.5 mm screw	10 (shear)	16 (withdrawal)	2	
		FT 4.5 mm screw			4	
Monotonic Compression (F4)	A90	PT 4.5 mm screw	10 (shear)	10 (-)	2	
		FT 4.5 mm screw			4	
	A105	PT 4.5 mm screw	10 (shear)	16 (-)	2	
		FT 4.5 mm screw			4	

2.4.1 Phase II – Test Setup

Figure 2.9 shows the test setup of cyclic uplift tests. The floor panel was held in place by two parallel rectangular hollow steel sections while the wall panel was clamped to the load cell. Due

to the restricted movement in compression, the loading protocol only included movements in the positive direction.

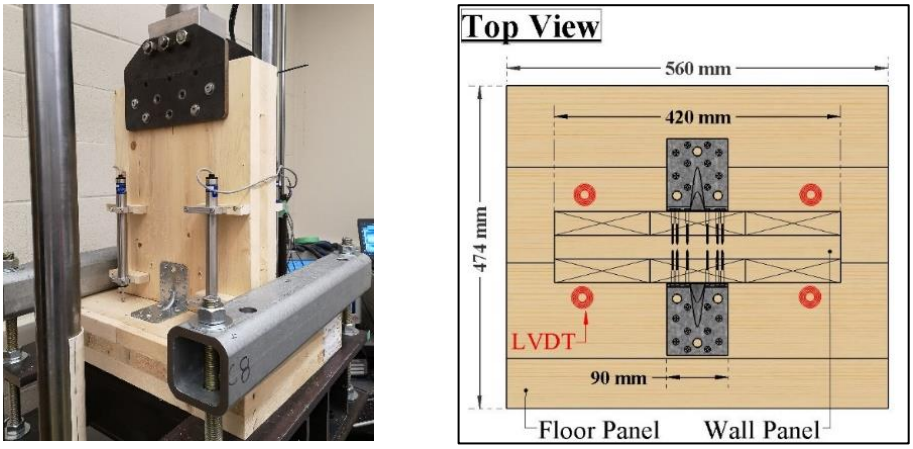

Figure 2.9. Cyclic uplift (F1) test setup: (a) test photo (with fixtures) and (b) top view.

Figure 2.10 shows test setups of cyclic in-plane shear tests. Similar to cyclic uplift tests, floor panels were held in place by two parallel rectangular hollow steel sections while wall panels were clamped at the top to the MTS testing machine. The out-of-plane rotation of the floor panels was controlled by the bottom and top plywood sheets attached to them (**Figure 2.10** a).

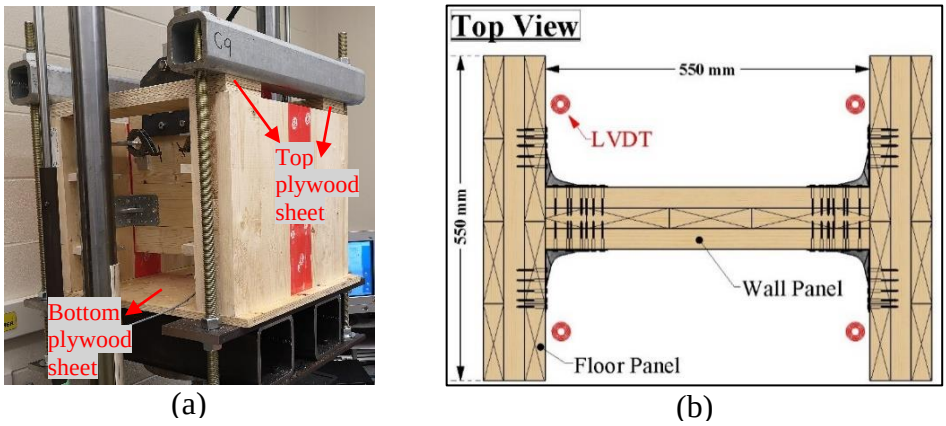

Figure 2.10. Cyclic in-plane shear (F2) test setup: (a) tests photo (with fixtures) and (b) top view.

Figure 2.11 shows test setups for both F3 (tension) and F4 (compression) tests. As **Figure 2.11** (a) shows, wall panels were set on top of rectangular hollow steel sections while the floor panel

was pushed down. The difference between tension and compression test setups is the position of angle brackets (**Figure 2.11** b and c).

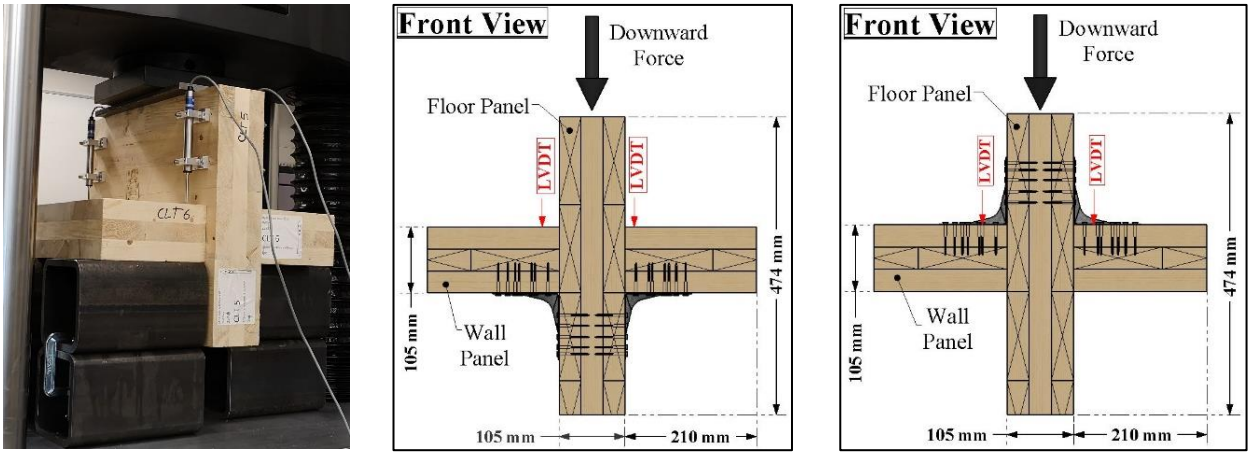

(a) (b) (c)

Figure 2.11. Monotonic out-of-plane tension (F3) and compression (F4) test setups: (a) F3 test photo (with fixtures), (b) front view of tension tests, and (c) front view of compression tests.

2.4.2 Phase II – Results and Discussion

Phase II test results were evaluated following the same procedure as Phase I. Additionally, ductility ratio (μ) and dissipated energy are calculated for cyclic tests following ASTM E2126 [42] procedure.

Phase II - F1 (cyclic uplift):

Figure 2.12 shows hysteresis loops and average backbone curves of Phase II – F1 tests and **Table 2.5** presents the mechanical properties achieved by the connections. All the hysteresis loops are highly pinched that reduces the energy dissipation of the connections. During the tests, screws attached to floor panels were progressively pulled out as the uplift displacement increased. Bracket size had little impact on the results since the capacity was governed by the same number of screws (10) in withdrawal. Changing the fasteners from partially-threaded to fully-threaded, however, increased the average yield and peak load by 12% and 11%, respectively, since a longer thread provided higher withdrawal capacity. Using fully-threaded screws also slightly increased the stiffness of the connections. Although the ductility factor of fully-threaded screw connections is smaller due to a relatively larger yield or smaller ultimate displacement, these connections dissipate 26% more energy in average compared to partially-threaded screw connections. The

bending moment caused by eccentricity in withdrawal force led to yielding and fracture of the embossed rib (**Figure 2.13** a), which propagated to the full cross-section of the bracket in some cases (**Figure 2.13** b). In such cases, screws closer to the rib were pulled out more than the ones closer to the far edge of the floor flange. Screws punching through the bracket was also observed in some cases (**Figure 2.13** a).

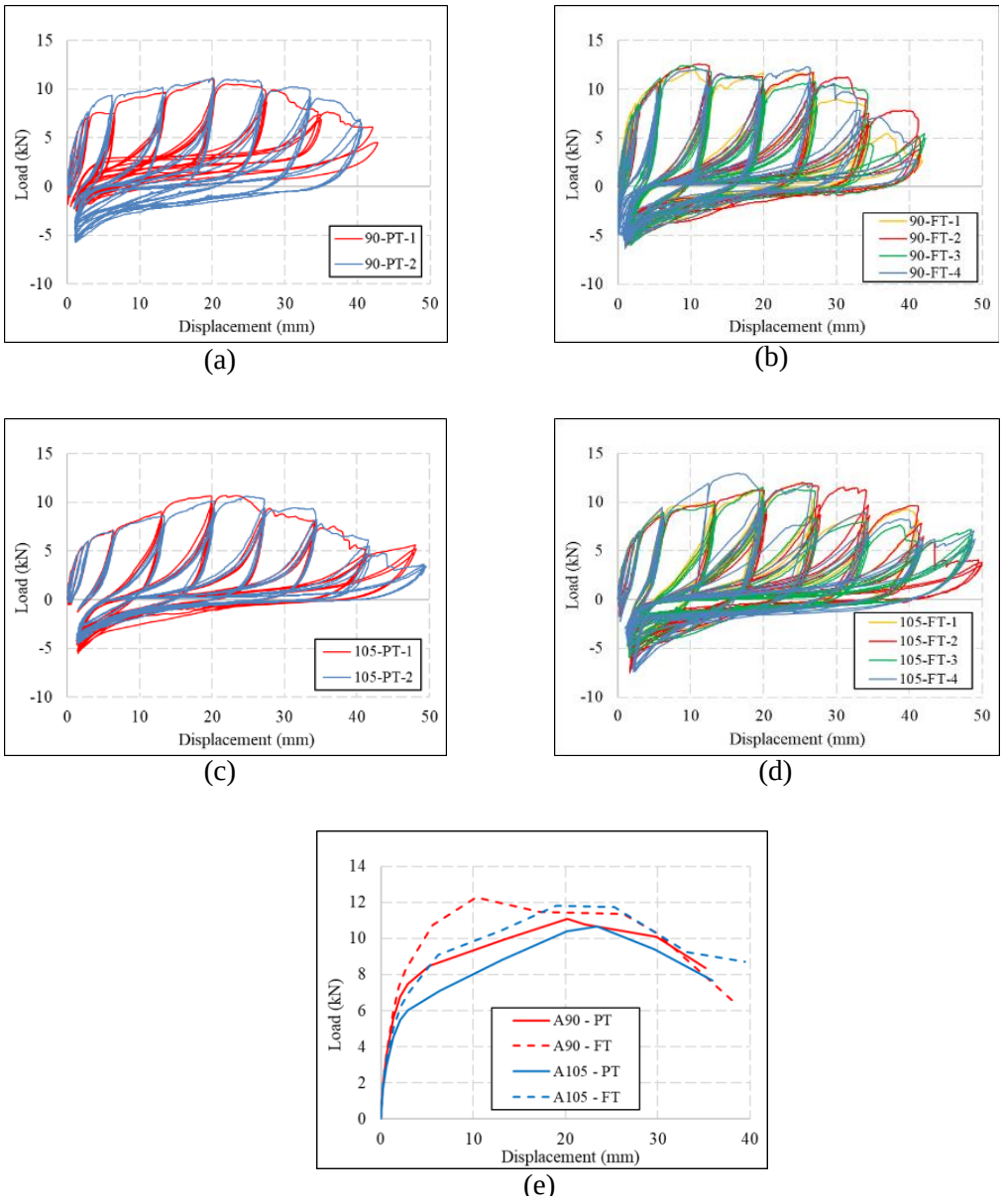

Figure 2.12. Load-displacement curves of Phase II - F1 tests: (a-d) Hysteresis loops and (e) backbone curves.

Table 2.5. Mechanical properties of angle bracket connections in Phase II - F1 tests.

Load Direction	Angle Bracket type	Screw thread type	+/-	Δ_y [mm]	P_y [kN]		Δ_{peak} [mm]	P_{peak} [kN]		Δ_u [mm]		P_u [kN]	K_{el} [kN/mm]		Ductility ratio (μ)[1]		Dissipated energy (E_d) [kN.mm]	
					Mean	COV		Mean	COV	Mean	COV		Mean	COV	Mean	COV	Mean	COV
Cyclic Uplift (F1)	A90	Partial	+	2.1	10.1	10.8%	20.2	11.1	1.3%	33.8	4.1%	8.9	4.7	1.6%	15.8	5.5%	1057	13.8%
		Full	+	2.1	11.2	4.2%	10.3	12.3	2.1%	31.1	5.2%	9.8	5.4	0.9%	15.0	4.6%	1313	6.3%
	A105	Partial	+	2.2	9.4	7.3%	23.4	10.7	0.5%	32.6	2.7%	8.5	4.2	2.5%	14.6	1.6%	979	2.6%
		Full	+	2.5	10.7	5.3%	21.8	12.1	4.5%	32.1	2.1%	9.4	4.3	3.5%	12.7	3.3%	1258	7.9%

Note: [1] The ductility is defined as the ratio of ultimate displacement over yielding displacement.

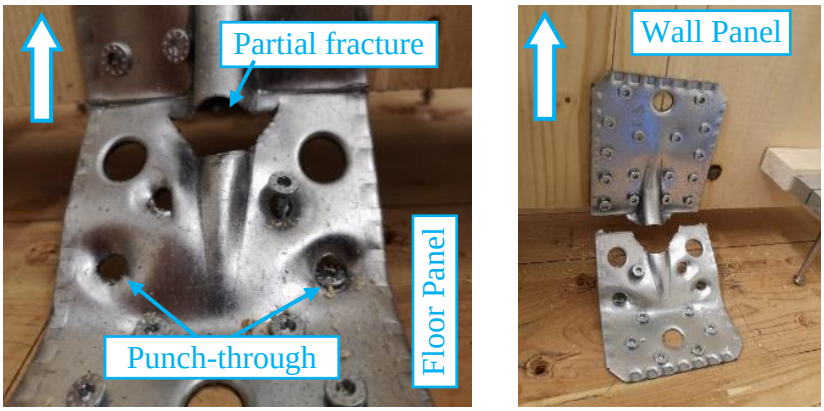

Figure 2.13. Failure modes in Phase II - F1 tests.

Phase II – F2 (cyclic in-plane shear):

Figure 2.14 shows hysteresis loops and average backbone curves of Phase II - F2 tests and **Table 2.6** presents the mechanical properties achieved by the connections. Large amounts of pinching in hysteresis loops lower the energy dissipation capacity of the connections. The relative shear displacement between wall and floor panels twisted the brackets and led to screw shear-off or pull-out (**Figure 2.15**). Using fully-threaded screws amplified the average yield and peak loads by 21% and 24%, respectively, and increased the stiffness of the connections (**Table 2.6**). Additionally, connections with fully-threaded screws dissipated 42% more energy than those with partially-

threaded screws. All tests failed due to a combination of brackets twisting and softening, screws pulling out, screw head shearing off, and the wall panels splitting (**Figure 2.15**).

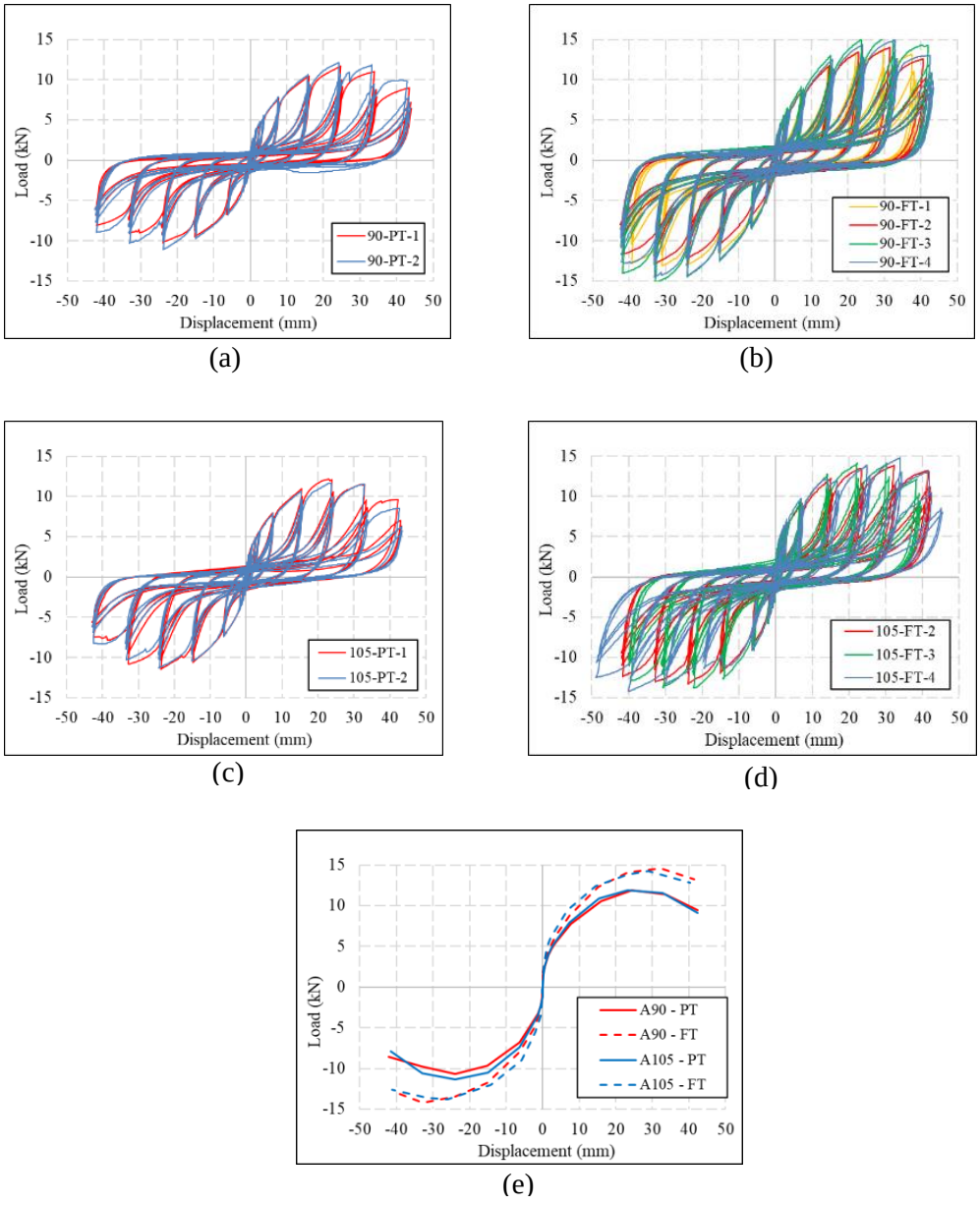

Figure 2.14. Load-displacement curves of Phase II – F2 tests: (a-d) Hysteresis loops and (e) backbone curves.

Table 2.6. Mechanical properties of angle bracket connections in Phase II - F2 tests.

Load Direction	Angle Bracket type	Screw thread type	+/-	Δ_y [mm]	P_y [kN]		Δ_{peak} [mm]	P_{peak} [kN]		Δ_u [mm]		P_u [kN]	K_{el} [kN/mm]		Ductility ratio (μ)		Dissipated energy (E_d) [kN.mm]	
					Mean	COV		Mean	COV	Mean	COV		Mean	COV	Mean	COV	Mean	COV
Cyclic Shear (F2)	A90	Partial	+	5.9	10.7	0.5%	24.5	11.9	1.8%	41.3	0.4%	9.6	1.8	2.1%	7.0	1.2%	2087	12.0%
			-	-5.2	-9.6	3.2%	-23.9	-10.7	3.9%	-42.3	0.5%	-8.6	1.8	6.9%	8.1	3.7%		
		Full	+	6.2	12.8	5.3%	32.2	14.6	5.0%	41.5	1.9%	13.2	2.1	1.1%	6.7	4.3%	3091	7.8%
			-	-5.9	-12.1	6.3%	-32.7	-14.2	5.1%	-41.2	1.5%	-12.8	2.1	0.7%	7.1	6.5%		
	A105	Partial	+	5.3	10.9	2.1%	23.4	11.9	1.9%	40.8	2.8%	9.5	2.1	5.9%	7.7	1.0%	2161	4.3%
			-	-4.9	-10.1	1.2%	-24.0	-11.4	1.2%	-37.2	0.9%	-9.1	2.1	6.3%	7.6	6.0%		
		Full	+	4.1	12.5	1.5%	28.9	14.3	2.7%	40.4	2.1%	12.8	3.1	5.9%	9.9	6.8%	2945	5.0%
			-	-4.1	-12.5	4.2%	-26.0	-13.8	2.6%	-41.1	1.8%	-12.5	3.1	6.0%	10.2	10.0%		

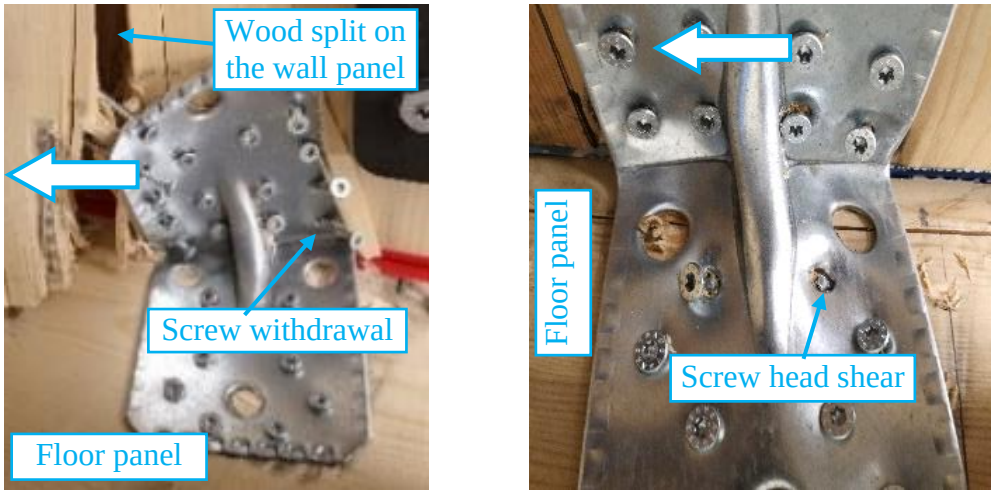

Figure 2.15. Failure modes in Phase II - F2 tests.

Table 2.5 and **Table 2.6** show that connections showed considerable strength and stiffness in both uplift and shear directions. Uplift tests achieved significantly higher ductility ratios than in-plane shear tests. The uplift ductility is almost two times the shear ductility (**Table 2.5** and **Table 2.6**). This is due to the higher initial stiffness of the uplift test leading to a smaller yield displacement compared to the shear test.

Phase II – F3 (monotonic out-of-plane tension):

Figure 2.16 shows the average load-displacement curves of Phase II - F3 tests. A105 brackets showed significantly higher strength than A90 brackets (**Table 2.7**) due to the greater number of screws working in withdrawal (16 in A105 and 10 in A90). All connections failed through CLT panels splitting under perpendicular to grain tension (**Figure 2.17** a), except A90 partially-threaded specimens that failed through the withdrawal of screws (**Figure 2.17** b). Specimens that failed due to splitting of wood had much smaller ultimate displacement than the ones that failed in screw withdrawal (**Figure 2.16**). The withdrawal of screws connected to the wall panel caused perpendicular to grain tension near the end of the wall. Splitting would occur when the total withdrawal force was increased beyond the wall end splitting resistance. The splitting of wall panels may become more critical due to the limited dimension of the wall panel along its major direction (210 mm) used in this project (**Figure 2.11**).

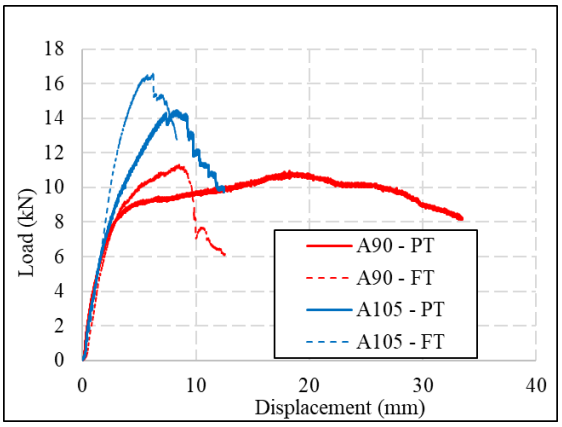

Figure 2.16. Load-displacement curves of Phase II - F3 tests.

Table 2.7. Mechanical properties of angle bracket connections in Phase II - F3 tests.

Load Direction	Angle Bracket Type	Fastener type	Δ_y [mm]	P_y [kN]		Δ_{peak} [mm]	P_{peak} [kN]		Δ_u [mm]		P_u [kN]	K_{el} [kN/mm]	
				Mean	COV		Mean	COV	Mean	COV		Mean	COV
Monotonic Tension (F3)	A90	PT	2.2	9.9	5.2%	18.5	10.9	5.7%	30.9	9.5%	8.7	4.5	5.8%
		FT	2.9	10.8	5.4%	8.5	11.3	1.4%	9.8	2.4%	9.0	3.7	7.2%
	A105	PT	3.0	13.4	4.8%	8.3	14.4	7.1%	10.3	11.5%	11.5	4.9	8.7%
		FT	3.1	15.1	3.2%	6.2	16.6	5.5%	8.1	6.5%	13.1	5.2	1.9%

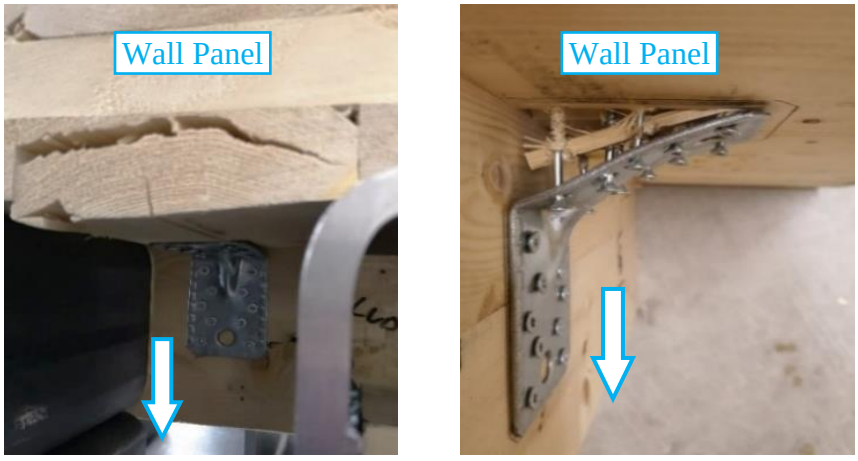

(a) (b)

Figure 2.17. Failure modes in Phase II -– F3 tests: (a) A90 brackets with fully-threaded screws and all A105 brackets in tension and (b) A90 brackets with partially-threaded screws in tension.

Phase II – F4 (monotonic out-of-plane compression):

Figure 2.18 shows the average load-displacement curves of Phase II – F4 tests. All specimens showed similar failure modes and achieved comparable strength values (**Table 2.8**). Failures initiated from the embossed rib in all brackets and led to a partial or full fracture of the bracket along with local crushing of wood material underneath the wall flange (**Figure 2.19**). The performance of the specimens mainly depended on the bracket size, with no correlations with the thread length of fasteners. **Figure 2.18** and **Table 2.8** show that A90 brackets exhibited larger ultimate displacement and higher ductility while A105 brackets exhibited greater stiffness, but lost strength faster. This is due to the larger flange width of the A105 (90 mm) bracket compared to the A90 bracket (65 mm) which led to less deformation on the bracket and wood panel in A105 connections under the same level of external force.

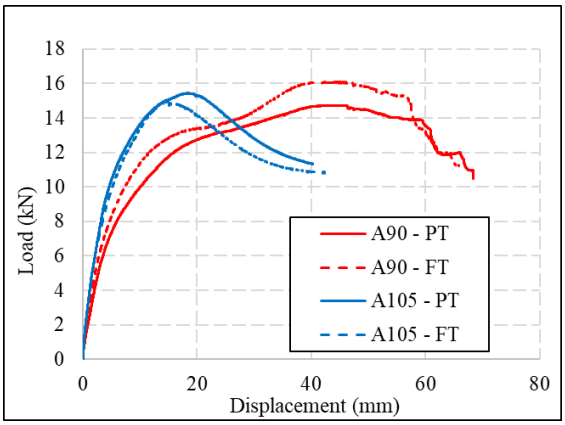

Figure 2.18. Load-displacement curves of Phase II - F4 tests.

Table 2.8. Mechanical properties of angle bracket connections in Phase II - F4 tests.

Load Direction	Angle Bracket Type	Fastener type	Δ_y [mm]	P_y [kN]		Δ_{peak} [mm]	P_{peak} [kN]		Δ_u [mm]		P_u [kN]	K_{el} [kN/mm]	
				Mean	COV		Mean	COV	Mean	COV		Mean	COV
Monotonic Compression (F4)	A90	PT	7.9	13.1	4.3%	46.2	14.7	1.9%	65.0	5.0%	11.7	1.7	6.0%
		FT	7.3	13.4	4.1%	44.0	16.1	5.6%	61.9	5.9%	12.8	1.8	3.0%
	A105	PT	4.7	14.1	2.0%	18.1	15.5	2.0%	31.9	5.5%	12.4	3.0	5.7%
		FT	4.4	13.7	1.2%	15.8	15.1	1.3%	28.1	1.8%	12.0	3.1	2.0%

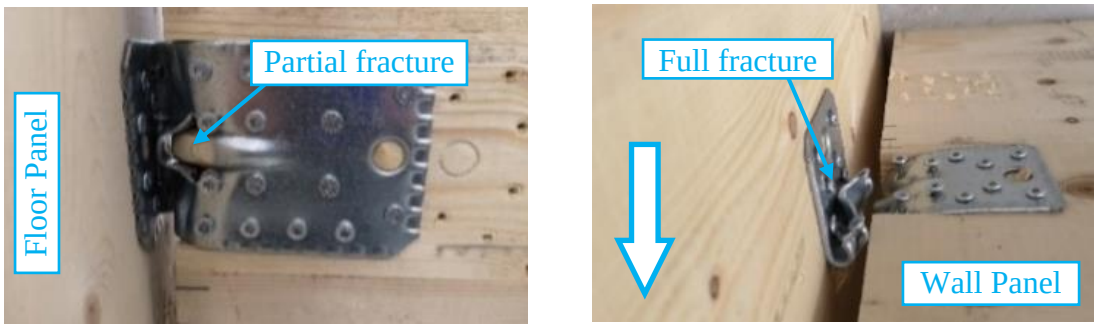

(a) (b)

Figure 2.19. Failure modes in Phase II - F4 tests: (a) partial fracture and (b) full fracture of the bracket.

2.5 Conclusion

A two-phase experimental study was carried out on a total of 60 monotonic and cyclic tests to assess the performance of CLT angle bracket connections. Two types of angle brackets (A105 and

A90) and four types of fasteners (12.7 mm screws, partially-threaded 4.5 mm screws, fully-threaded 4.5 mm screws, and threaded 4.5 mm ring nails) were used to assemble the specimens. Specimens were tested under in-plane and out-of-plane loading scenarios in four directions. The average mechanical properties are reported for every set of tests along with their coefficient of variations (COVs). All data sets have a COV lower than 15% with the vast majority of them under 10%. The low COVs of test data is probably due to the averaging effect of multiple fasteners in one angle bracket connection and multiple connections in one specimen in a symmetric test setup.

Phase I results show that small diameter fasteners are more desirable for wood-to-wood angle bracket connections in terms of failure modes, load-bearing capacity and stiffness. Therefore, 4.5 mm screws were chosen due to their desirable uplift and in-plane shear performance and easy assembly process. The following conclusions were derived from Phase II tests:

- In-plane cyclic uplift and shear tests failed largely in ductile manners due to combinations of yielding of brackets and yielding or pull-out of screws. Splitting of CLT panels was captured in few tests in large displacements. High ductility and energy-dissipation were achieved in both uplift and in-plane shear directions. In this research, specimens were only loaded in one direction. Further research on the performance of angle bracket connections loaded in multiple directions is needed to investigate the effect of load combinations.
- Out-of-plane tension tests primarily failed in the splitting of CLT panels under perpendicular to grain tension, except A90 brackets with partially-threaded screws that exhibited ductile failures due to screw withdrawal. A105 brackets showed significantly higher strength than A90 brackets in tension. Out-of-plane compression tests, however, exhibited ductile failures. The two sizes angle brackets achieved comparable strength, with more ductility captured in A90 samples. Since wind and seismic load can induce both out-of-plane tension and compression to angle bracket connections, these connections should be designed within elastic range to avoid the brittle failure.
- Angle brackets with fully-threaded screws exhibit higher strength and stiffness and dissipated more energy than angle brackets with partially-threaded screws in uplift, in-plane shear and out-of-plane tension tests. However, angle brackets with partially-threaded screws exhibited more ductile performance in some cases.

Further studies will investigate the performance of angle bracket connections under multi-directional loads through numerical modelling analysis. Using combinations of fasteners to achieve better mechanical properties is also worth investigating.

Chapter 3: Numerical analysis of in- and out-of-plane coupling effects on angle bracket connections in CLT structures

3.1 Introduction

Cross laminated timber (CLT) structures are gaining more attention and achieving new heights in North America [14], [15]. Due to the brittle nature of wood, CLT structures rely on metal connections to achieve required ductility and energy dissipation [1]–[4], [6]. When designed properly with steel connectors and CLT elements, the structure can exhibit superior seismic performance by leveraging the high strength-to-weight ratio of wood members and the high ductility of steel components [1], [16], [21], [44]. A good understanding of connections in CLT structures is needed to better predict the performance of the structures and avoid brittle failure mechanisms [1], [2], [22], [23].

Steel angle brackets, hold-downs, and self-tapping screws are the most widely-used connectors in CLT structures [2]. Many studies have focused on the performance of such connections in CLT systems [1], [2], [37]–[39], [3], [8], [20], [21], [27], [30], [34], [35] with the assumption that hold-downs and angle bracket connections work solely in their primary directions, i.e. hold-downs in uplift and angle bracket connections in shear [21], [38]. D'Arenzo et al. [38] consider hold-downs work only in uplift to control the rocking behavior of the system, while angle bracket connections work mainly in shear to prevent sliding mechanism under wind or seismic loads. Other studies, however, recognize the contribution of these connections in both their primary and secondary directions [1], [2], [20], [27], [34]. Gavric et al. [27] studied the behavior of angle bracket connections in both shear and uplift directions under monotonic and cyclic loads and concluded that angle bracket connections offered significant strength and stiffness in both directions. Flatscher et al. [39] and Casagrande et al. [34] achieved the same results as Gavric et al. [27] by testing different types of angle bracket connections in shear and uplift directions.

For both assumptions aforementioned, the effect of uplift on the shear performance of CLT angle bracket connections needs to be investigated unless the uplift force can be released. Liu and Lam [37] tested the connections under monotonic and cyclic shear loadings, with four different levels

of constant uplift forces applied simultaneously. They found that shear and uplift performance are strongly coupled for such connections and the shear strength and stiffness of the connection decreases considerably in the co-existence of uplift force. Liu and Lam [45] carried out a similar study for CLT hold-down connections and observed that the co-existence of shear load weakens the axial performance of the connections at large vertical displacements. Later, Liu et al. [46] used the HYST algorithm, a protocol-independent procedure, to reproduce their experimental findings on the coupling effects of biaxial loading on the performance of CLT connections. In the HYST algorithm, the nail shank was modeled as a steel beam element, and the wood embedment medium was modeled as compression-only spring elements. Pozza et al. [25], [30] performed experimental tests on CLT angle bracket and CLT hold-down connections under biaxial shear-uplift loads. They concluded that the shear capacity of angle-bracket connections and uplift capacity of hold-downs decrease with the co-existence of uplift and shear loads, respectively. They, later, proposed a finite element model using OpenSees to simulate the uplift-shear behavior of angle bracket and hold-down connections under simultaneous application of the biaxial forces. D'Arenzo et al. [4] developed a detailed 3D finite element model of angle bracket connections in ABAQUS. In their study, the fasteners were simplified as two-node non-linear spring elements, able to simulate the non-linear behavior under monotonic load, and pinching, stiffness and strength degradation under cyclic loads. The model was verified by reproducing the results of the experimental tests, and then used to analyze the coupled uplift-shear behavior of CLT angle bracket connections. They exerted an inclined displacement to the connection in 15° intervals starting from 0° (only shear) to 75° and found that the co-existence of an uplift force reduces the shear strength of the connection.

The above-mentioned studies are mainly focused on the in-plane performance of CLT connections. In reality, these connections may also experience out-of-plane movements under wind and seismic loads. There is a lack of research to address the effect of out-of-plane forces on the in-plane resistance of angle bracket connections. In the earlier research, Rezvani et al. [2] carried out a comprehensive experimental campaign on CLT angle bracket connections through monotonic and cyclic tests in four in- and out-of-plane directions. They found that the connections offered considerable strength and stiffness in the primary direction (in-plane shear) as well as secondary directions (in-plane uplift and out-of-plane tension and compression). In this paper, the coupling effect on CLT angle bracket connections under both in- and out-of-plane directions is studied through two-phase numerical modeling analysis. In Phase I, a 3D finite element model was

developed in ABAQUS and verified with the experimental results obtained in the previous study by the authors [2]. In Phase II, the verified model was used to simulate the behavior of connections under biaxial loads. The novelty of this study is two-fold. First, out-of-plane tension and compression loads are included as the secondary load directions for angle bracket connections. Second, different from previous studies that a two-node non-linear spring element was usually used to simulate the behavior of angle bracket connections, this study developed a detailed 3D model for all parts, including fasteners, and considered the interactions between the fasteners and the wood material. This 3D modeling approach can provide a better prediction of the failure mechanisms of angle bracket connections in biaxial loading scenarios.

3.2 Development of 3D Numerical Models

In the previous study, Rezvani et al. [2] tested two types of angle brackets (i.e. A90 and A105) and four types of fasteners (i.e. 12.7 mm screw, partially-threaded 4.5 mm screw, fully-threaded 4.5 mm screw, and threaded 4.5 mm ring nail). This study is based on test results of connections with A105 angle bracket and fully-threaded 4.5 mm screws. This section describes the details of the developed 3D model and its verification process.

3.2.1 Model Description

In contrast to the existing literature on numerical simulations of the biaxial performance of angle bracket connections, all parts of the connections are modeled with 3D elements. Although it results in increased analysis time, 3D elements would better model the stress and strain development on each component and the interactions between them, therefore better predicting the deformations and failure modes of the connections under biaxial loading conditions.

The 3D ABAQUS model, shown in **Figure 3.1**, consists of three distinct parts: A105 angle bracket (105 × 90 mm flanges, asymmetric configuration with 10 small (ϕ 5 mm) and three big (ϕ 13 mm) holes on one flange and 16 small and one big hole on the other flange), fully-threaded 4.5 × 50 mm screws, and CLT panels. Simplified versions of the parts were used to optimize the analysis time while maintaining the accuracy of the model. For example, the screw (**Figure 3.1** b) was modeled with a 4.5 mm smooth shank (no thread), and the 3-ply panels were reduced to 2-ply

panels since the screws only penetrated into two layers and the third layer did not impact the results.

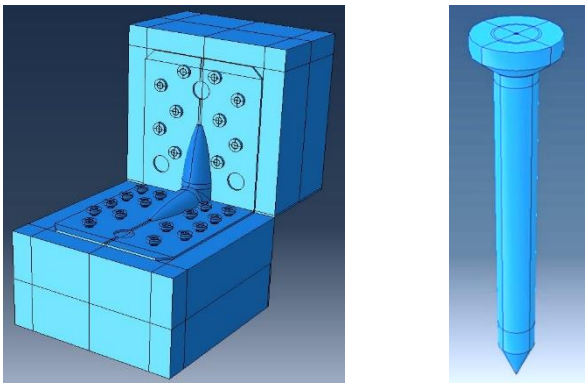

(a) (b)

Figure 3.1. ABAQUS model: (a) whole connection, and (b) screw.

The material properties [47], [48] of Douglas-Fir CLT panels are shown in **Table 3.1**. Hashin failure criterion was used in this project to model the anisotropic performance of wood [47]. This method was originally developed to model fiber-reinforced composites [49], [50] and can simulate material softening and failure in a ductile or brittle manner. In the Hashin material model, the material softening rate is specified by the fracture energy of the material [47]. As required by the Hashin material model in ABAQUS, quadrilateral continuum shell elements (SC8R) were used to create CLT layers. These elements are suitable for nonlinear geometric analysis since they allow material deformation and rotation in all three dimensions [51]. The layers were then stacked crosswise to create the CLT panels. Two methods were tried to create bonding between wood layers in CLT panels: cohesive surface and tie constraint. The two methods provided similar results; therefore, the tie constraint method was chosen due to being significantly less time-consuming.

Table 3.1. Material properties of Douglas-Fir (Hollenbeck, 2018; Kretschmann, 2010).

Linear-elastic properties*		Failure criteria (MPa)		Fracture energy (N/mm)	
E11 (MPa)	14700	Parallel Tension	108	Longitudinal Tension	1.6
E22 (MPa)	737	Parallel Compression	29.8	Longitudinal Compression	60
E33 (MPa)	1000	Matrix Tension	2.3	Transverse Tension	0.06
Nu12	0.449	Matrix Compression	5.5	Transverse Compression	0.2
Nu13	0.292	Longitudinal Shear	7.8		
Nu23	0.374	Transverse Shear	7.8		
G12 (MPa)	1150				
G13 (MPa)	942				
G23 (MPa)	103				

*Directions 11, 22, and 33 in the table refer to longitudinal, tangential, and radial directions of the lumber, respectively.

The angle bracket and screws were modeled as isotropic elastoplastic material with strain-hardening behavior [40], [52]. **Table 3.2** presents material properties for the angle bracket and screws. Both parts were modeled using linear brick elements with reduced integration (C3D8R) to increase the computational efficiency without losing accuracy [51].

Table 3.2. Material properties of angle bracket and screws [40], [52].

Part	Density (Kg/m^3)	Elastic modulus (MPa)	Yield strength (MPa)	Ultimate strength (MPa)	Poisson ratio
Angle bracket	8,000	200,000	250	330	0.30
Screw	8,000	200,000	215	450	0.29

In ABAQUS, contact modeling is divided into two segments: normal (e.g., pressure and adhesion) and tangential (e.g., friction). In this connection model, normal contacts were defined as hard contact which works well for modeling interactions between solid materials. It relies on the pressure-overclosure method between surfaces and material properties of each part to prevent overlaps between them. Additionally, tangential contacts were modeled using the penalty method which relies on normal-to-surface force and friction coefficient to simulate frictional behavior in the model. Since the screw shank was modeled as a smooth (unthreaded) surface, the withdrawal resistance of the screw depended solely on its friction to the surrounding wood material. To create a normal force in the model, CLT panels were pre-drilled and the hole was one millimeter smaller than the diameter of the screw shank. Therefore, the insertion of screws in the panels created the normal force necessary for frictional behavior. Static-Kinetic Exponential Decay frictional model

was used in which the friction was defined by three factors, i.e., static coefficient, decay coefficient, and kinetic coefficient [51]. To find the proper friction coefficients, a set of withdrawal tests were carried out on the fully-threaded 4.5 × 50 mm screws. The test setup (**Figure 3.2**) included a piece of CLT member clamped at two ends and a steel slot to clamp the screw head. The screw was pre-inserted to the CLT piece and pulled out at a rate of 2 mm/min according to ASTM D1761 [53].

(a) (b) (c)

Figure 3.2. Screw withdrawal test: (a-b) test device and setup, and (c) fully-threaded 4.5 × 50 mm screw.

A 3D numerical model (**Figure 3.3** a) was created with the aforementioned modeling approaches to simulate the screw withdrawal performance. The numerical results were then compared with the average results of the experimental test (three replicates). A good fitting was achieved when the static, kinetic, and decay coefficients were set to be 1.6, 0.3, and 4.0, respectively (**Figure 3.3** b), although a slightly higher displacement at peak load and a more gradual softening behavior was observed in the model. Therefore, this set of friction coefficients were used for verification of modelling approach, and analysis of angle bracket connections under biaxial loads.

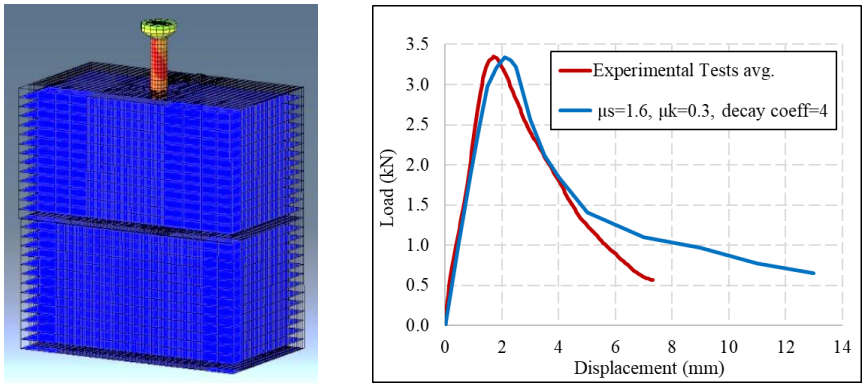

(a) (b)

Figure 3.3. Withdrawal performance: (a) numerical model, and (b) comparison between numerical and experimental tests.

A mesh sensitivity analysis was carried out to find the optimum mesh size for the model. Based on the analysis, a mesh size of 0.5 mm was chosen for all parts. All elements were set to be deleted after fully losing their strength, at which point their contribution to the system is negligible. Non-linear, dynamic explicit, displacement-controlled analyses were performed and the mass-scaling technique was used to increase the analysis speed.

3.2.2 Model Verification

Experimental monotonic tests conducted by Rezvani et al. [2] were used to verify the developed modeling approach in four directions: in-plane uplift (F1 in **Figure 3.4**), in-plane shear (F2 in **Figure 3.4**), out-of-plane tension (F3 in **Figure 3.4**), and out-of-plane compression (F4 in **Figure 3.4**). The directions are shortened to shear, uplift, tension, and compression in the rest of this article. One model (**Figure 3.1**) was used for all four directions, but boundary conditions and loading direction were customized for each case. Equivalent energy elastic-plastic (EEEP) curves were developed based on load-displacement curves of numerical modeling results according to ASTM E2126 [42] and used to determine the mechanical properties of connections including the yield load (P_y), displacement at yield (Δ_y), peak load (P_{peak}), displacement at peak load (Δ_{peak}), ultimate displacement (Δ_u), ductility ratio (μ), and stiffness (k).

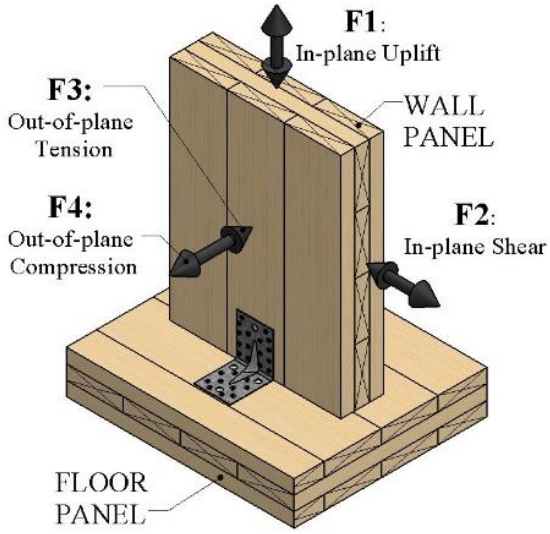

Figure 3.4. Loading directions in CLT angle bracket tests (Rezvani et al., 2021a).

Figure 3.5 shows the comparison of failures modes of numerical models with those observed in experimental tests in each loading direction. A high level of similarity exists between experimental and numerical deformations and failure modes. Although wood splitting in the out-of-plane tension test (F3 in **Figure 3.4**) could not be exhibited with the adoption of continuum shell elements in ABAQUS, tensile failure was observed on wood (red area in **Figure 3.5 c**). Similarly, **Figure 3.6** and **Table 3.3** compare load-displacement curves and mechanical properties achieved by numerical models with those of experimental tests in each direction. The experimental and numerical curves align closely before reaching their peak, and only limited deviations are observed after that point. The models show slightly higher peak (3.7~5.3%) and yield (4.7~7.6%) loads compared to the test results as well as higher ultimate displacements (4.5~14.7%). On the other hand, numerical models achieved lower stiffness and ductility ratio in F1, F2, and F3 directions, but higher in the F4 direction. This may be due to the differences that F4 tests mainly rely on the angle bracket(s) performance while the other tests rely largely on the fastener (screw) behavior. Overall, the numerical model shows high accuracy, and therefore, will be used to evaluate the behavior of angle bracket connections under biaxial loads.

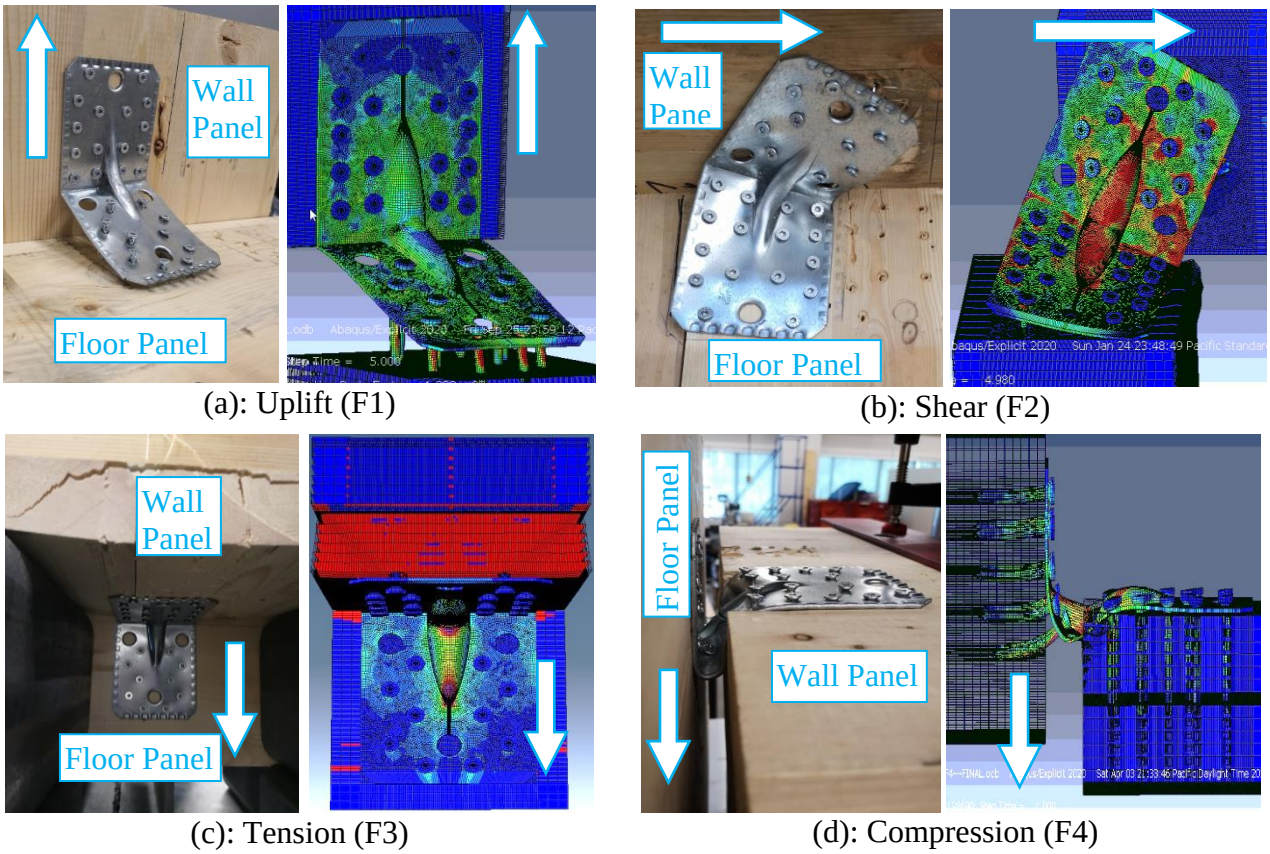

(a): Uplift (F1)

(b): Shear (F2)

(c): Tension (F3)

(d): Compression (F4)

Figure 3.5. Comparison of deformations and failure modes between experimental tests and numerical models.

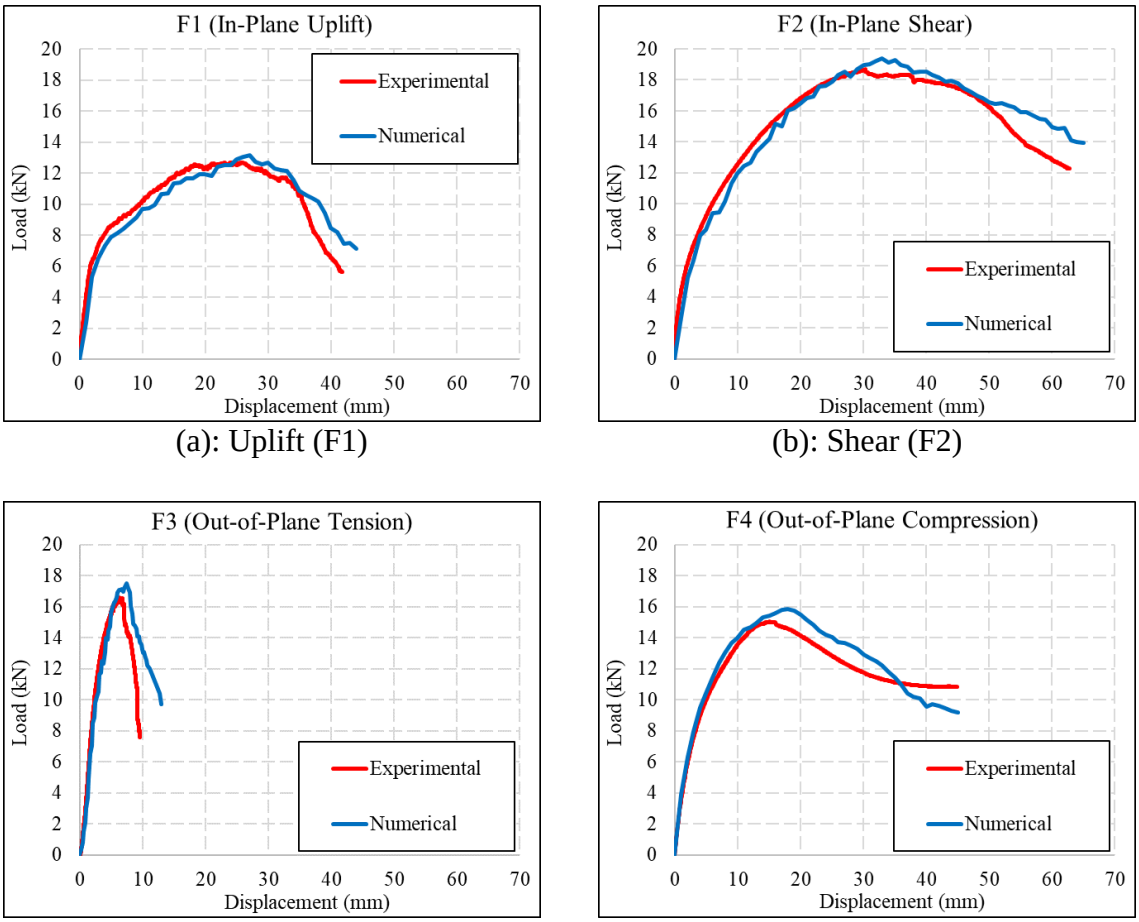

(a): Uplift (F1) (b): Shear (F2)

(c): Tension (F3) (d): Compression (F4)

Figure 3.6. Comparison of load-displacement curves between experimental tests and numerical models.

Table 3.3. Mechanical properties of numerical models (mean values) and their error compared to experimental results [Err%]

Load direction	Δ_y [mm]	P_y [kN]		Δ_{peak} [mm]	P_{peak} [kN]		Δ_u [mm]		K_{el} [kN/mm]		Ductility ratio (μ)	
		Mean	Err [%]	Mean	Mean	Err [%]	Mean	Err [%]	Mean	Err [%]	Mean	Err [%]
Uplift (F1)	3.5	11.5	4.7	27.0	13.3	4.3	36.5	4.5	3.3	-12.9	10.4	-13.0
Shear (F2)	7.5	17.5	5.9	33.0	19.4	3.7	57.6	7.8	2.3	-7.9	7.7	-5.9
Tension (F3)	3.7	17.0	5.4	7.5	17.5	5.3	9.5	14.7	4.6	-11.8	2.6	-2.2
Compression (F4)	4.2	14.9	7.6	18.0	15.9	5.0	31.4	10.6	3.7	10.6	7.4	13.6

3.3 Performance of Angle Bracket Connections under biaxial Loads

The verified numerical model was used to assess the performance of CLT angle bracket connections under biaxial loads. According to Pozza et al. [25], different protocols may be

followed to load the connections in multiple directions. The two most common protocols are "simultaneous" and "sequential". In the "simultaneous" protocol, a combined load is applied at a specific angle following the pre-defined rules, and the connection is loaded in multiple directions simultaneously (see e.g. [4]). The angle of the load determines the load component in each direction. In the "sequential" protocol, the main goal is to study the response of the system along the primary direction with the co-existence of the secondary direction load. In this protocol, the displacements imposed along the secondary directions are maintained constant throughout the simulation process. Since angle brackets are primarily designed to withstand shear loads, this study followed the "sequential" protocol to assess the performance of the connections along the shear direction (F2 in **Figure 3.4**) after different levels of constant displacements applied along uplift, tension, and compression directions (F1, F3, and F4 in **Figure 3.4**), respectively. The "sequential" loading protocol was carried out in two steps:

1. **Initial displacement:** An initial displacement was imposed to the connection along one of the secondary axes. Displacement values were chosen in a way that the corresponding forces were 25, 50, 75, and 100% of the monoaxial peak load in the respective direction.
2. **Primary displacement:** A primary displacement was imposed to the connection along the shear direction up to 70 mm while the initial displacement along the secondary direction was maintained constant. The 70 mm threshold was chosen based on the load-displacement curve of the shear (F2) model.

Table 3.4 shows the three sets of numerical models simulated to assess the impact of prescribed initial displacements along the secondary directions on the shear performance of angle bracket connections. The F2-F1 coupling happens when rocking and slip mechanisms act jointly on the connections [37]. Similarly, F2-F3 and F2-F4 combinations happen when wind and seismic loads impose both in- and out-of-plane loads to the connections.

Table 3.4. Biaxial numerical models

Loading set	Initial displacement			Primary displacement		Scenario description
	Direction	Δ [mm]	% of P_{peak} induced	Direction	Δ [mm]	
F2-F1	F1	1.5	25	F2	70	Combined rocking and slip mechanism
		3.0	50			
		12.0	75			
		27.0	100			
F2-F3	F3	1.5	25	F2	70	Combined wind and seismic loads
		2.5	50			
		4.0	75			
		7.5	100			
F2-F4	F4	1.0	25	F2	70	Combined wind and seismic loads
		3.0	50			
		6.5	75			
		18.0	100			

Figure 3.7 , **Figure 3.8**, and **Table 3.5** show the load-displacement curves, failure modes, and mechanical properties of the angle bracket connections under biaxial loads, respectively. It can be seen that the application of initial displacements in the secondary directions significantly impacts the performance of the connections in shear (**Figure 3.7**). When the initial displacement induced 25% of P_{peak}, the failure modes of angle bracket connections under biaxial loads are similar to that under monoaxial loads, including the combinations of twist and yielding of brackets, and yielding or pull out of screws (**Figure 3.8**). However, at higher levels of initial load (i.e. 50%, 75%, and 100%), failure modes vary due to the impact of initial displacement. F2-F1 and F2-F4 combinations experienced a partial fracture in the bracket rib during the initial loading, which turned into a full fracture upon the application of shear (F2) load. Similarly, F2-F3 combination experienced the full fracture after the shear load was applied, but without experiencing any partial fractures during the initial loading. The full fracture was not seen in shear-only tests, which means that the application of tension (F3) load affected the failure mode. **Table 3.5** shows the ratio of mechanical properties achieved by biaxial models to the ones achieved by the shear only (F2) model. Overall, as the initial displacement increased, connections achieved lower yield and peak loads, as well as smaller displacements at yield and peak. Similarly, stiffness and ultimate displacement of the connections decreased with the increase in initial displacements. More

specifically, the co-existence of secondary load has limited effect on shear performance of angle bracket connections when the initial displacement induced 25% of P_{peak} in the secondary direction. When the initial load increased to 50%, 75% and 100% of P_{peak}, the shear resistance reduced around 10%, 30% and 60%, respectively. The results align with the findings of Liu and Lam [37] in their study of shear-uplift coupling effects on angle bracket connections. Although load-displacement curves and mechanical properties changed similarly across numerical model sets, failure modes varied among them. Overall, both F2-F1 and F2-F4 model sets lost strength gradually after the peak load and in ductile manners with little to no sign of sudden, brittle failures (**Figure 3.8** a, c). On the other hand, most F2-F3 models lost strength quickly after reaching their peak shear resistance, especially when the secondary load was increased beyond 75% of its resistance (**Figure 3.8** b). The difference in connection performance under F2-F1 and F2-F3 loads is due to the different number of fasteners used in the angle bracket connections for resisting the withdrawal force (10 screws in F2-F1 and 16 screws in F2-F3). In both loading scenarios, the withdrawal of screws induced perpendicular to grain tension to CLT panels. When the withdrawal resistance of screws is larger than that of the perpendicular to grain tension, such as the F2-F3 case, the connections failed in much smaller ultimate displacement due to the split of wood. Additionally, although higher levels of initial displacements led to a decline in ductility ratio in F2-F1 and F2-F3 model sets, the decline was not as pronounced as that of other mechanical properties. The ductility ratio of F2-F4 case did not follow the same trend.

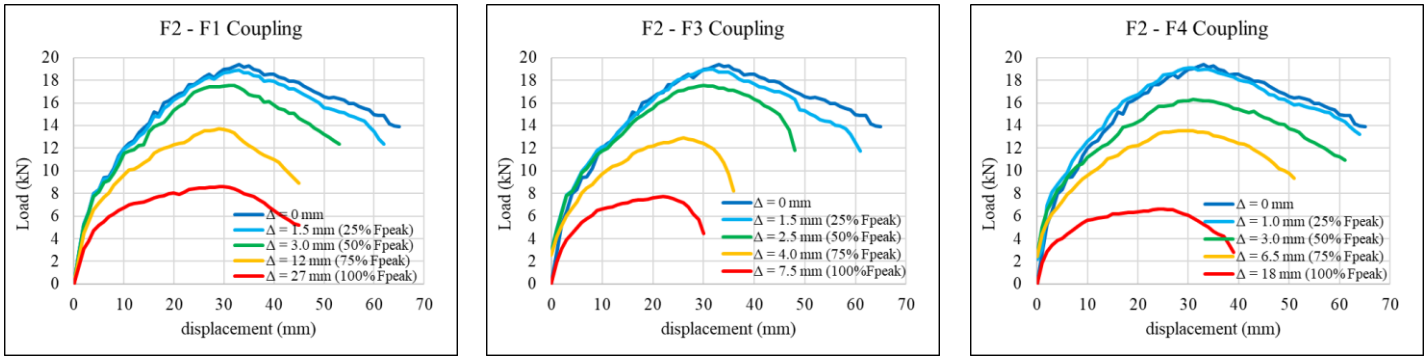

(a): F2-F1 set (b): F2-F3 set (c): F2-F4 set

Figure 3.7. Load-displacement curves of biaxial numerical models.

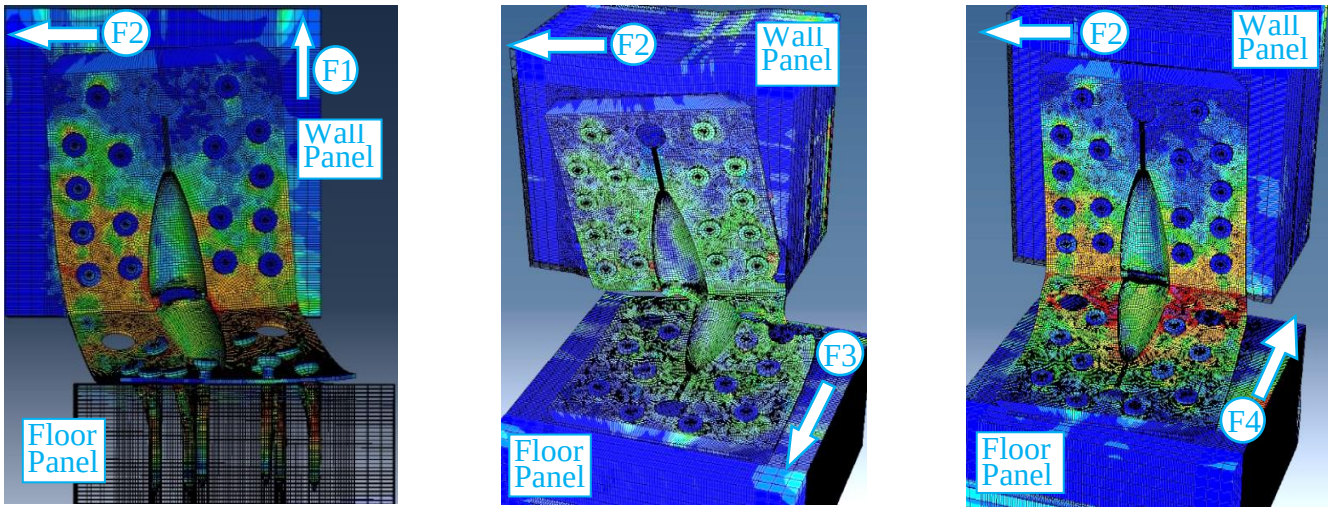

(a): F2-F1 set (b): F2-F3 set (c): F2-F4 set

Figure 3.8. Failure modes of biaxial numerical models.

Table 3.5. Mechanical properties of biaxial numerical models

Load set	Initial stage			Primary stage						
	Loading Direction	Δ [mm]	% of P_{peak} induced	Δ_y [mm]	P_y [kN]	Δ_{peak} [mm]	P_{peak} [kN]	Δ_u [mm]	K_{el} [kN/mm]	Ductility ratio (μ)
F2 only	-	-	-	7.5	17.5	33.0	19.4	57.6	2.3	7.7
F2-F1	F1	1.5	25	7.5	17.1 (98%) *	33.2	18.9 (98%)	54.2 (94%)	2.3 (97%)	7.2 (94%)
		3.0	50	7.5	16.1 (92%)	32.0	17.5 (90%)	47.4 (82%)	2.2 (92%)	6.4 (83%)
		12.0	75	6.9	12.7 (73%)	28.9	13.8 (71%)	40.0 (69%)	1.8 (78%)	5.8 (75%)
		27.0	100	6.6	7.5 (43%)	29.1	8.6 (44%)	38.6 (67%)	1.1 (49%)	5.8 (76%)
F2-F3	F3	1.5	25	7.5	17.6 (101%)	32.4	19.0 (98%)	50.4 (88%)	2.4 (101%)	6.8 (88%)
		2.5	50	6.8	15.8 (90%)	29.8	17.5 (90%)	46.3 (80%)	2.3 (99%)	6.8 (88%)
		4.0	75	6.7	11.7 (67%)	26.2	12.9 (66%)	34.3 (60%)	1.7 (74%)	5.1 (67%)
		7.5	100	6.5	7.0 (40%)	22.0	7.7 (40%)	28.0 (49%)	1.1 (46%)	4.3 (56%)
F2-F4	F4	1.0	25	7.4	17.8 (102%)	30.5	19.1 (99%)	56.4 (98%)	2.4 (103%)	7.7 (100%)
		3.0	50	6.7	14.7 (84%)	31.1	16.3 (84%)	52.9 (92%)	2.2 (94%)	7.9 (102%)
		6.5	75	6.0	12.2 (70%)	29.9	13.5 (70%)	46.4 (81%)	2.0 (87%)	7.7 (100%)
		18.0	100	3.8	6.0 (34%)	25.1	6.7 (34%)	32.9 (57%)	1.6 (67%)	8.6 (112%)

* Values in prentices indicate the ratio of the value over F2 only results.

3.4 Comparison with Analytical Model

The European Technical Assessment (ETA) 08/0183 [40] predicts that when combined forces act on the angle bracket connections, the following inequality shall be fulfilled:

$$\sum_{i=1}^{n} \left(\frac{F_i}{F_{i,max}} \right)^2 \leq 1 \quad (1)$$

where i is the direction of the load and F_i is as shown in **Figure 3.8**. The interaction shown in Eq. (1) provides a perfect quarter-oval-shape strength domain for every coupled direction. The length of each axis of the oval depends on the peak strength of the connection under monoaxial load in each direction. **Figure 3.8** shows a comparison between numerical results from this study and those calculated with the ETA-08/0183 analytical formula [40]. As shown, most of the data points are well aligned with the quarter-oval strength-domain boundary, meaning that Eq. (1) can well predict the coupling effect of secondary loading on the shear resistance of angle bracket connections, except that when the initial load equals the peak load in the secondary direction, Eq. (1) lower estimates the shear resistance.

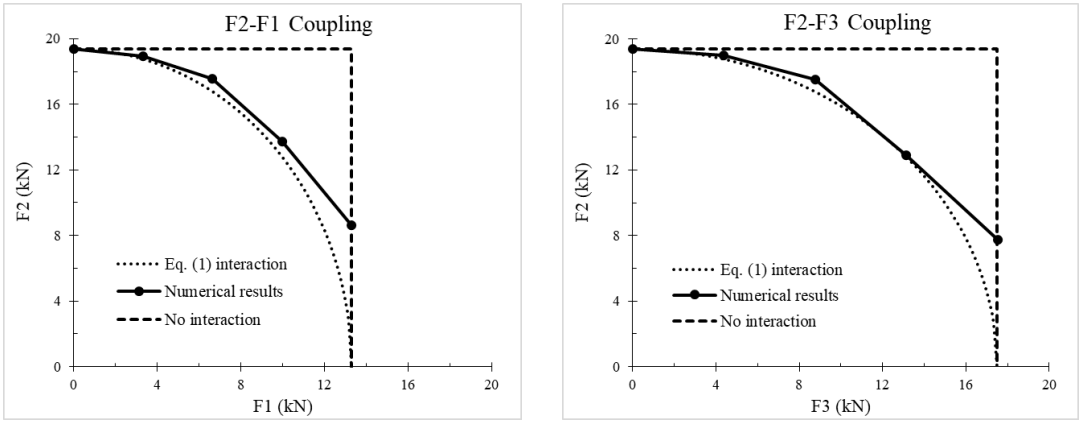

(a): F2-F1 set (b): F2-F3 set

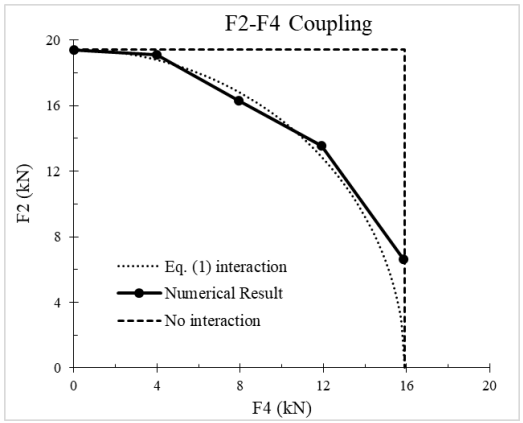

(c): F2-F4 set

Figure 3.9. Comparison of numerical results with ETA analytical model predictions (European Technical Assessment, 2018).

3.5 Conclusion

A two-phase numerical study was carried out using ABAQUS software to investigate the performance of CLT angle bracket connections under biaxial loads. The fasteners were modeled with 3D elements being able to simulate the interactions between the fastener and its surrounding media, and the failure modes of connections under biaxial loads.

In Phase I, a wall-to-floor angle bracket connection model was developed and verified with the results of experimental tests previously conducted by the authors [2]. The numerical model was loaded in four directions: uplift, shear, tension, and compression (F1 to F4 in **Figure 3.8**, respectively), and the results were compared with the test data. Most of the average errors in mechanical properties between numerical modelling analysis and experimental study fall within

10% which indicates that the developed 3D model can well predict the performance of angle bracket connections under in- and our-of-plane loads.

In phase II, the verified models were used to evaluate the biaxial performance of the connections. The connections were loaded in two sequential steps. First, four levels of initial displacements (relative to 25%, 50%, 75% and 100 % of peak load) were applied to the connection along a secondary direction (i.e., F1: uplift, F3: tension, or F4: compression). Then, the connections were loaded up to 70 mm displacement along the shear (F2) direction in all cases. The performance of the connections under biaxial loads was evaluated in terms of strength, stiffness, ductility ratio, and failure modes, and compared with the shear performance of connections without initial loading. Results show that the co-existence of in-plane uplift, and out-of-plane tension and compression forces reduced the shear strength, stiffness, and ultimate displacement of angle bracket connections, while the failure modes were similar to that under shear load only. Results from the numerical model indicate that the shear performance of the connections is strongly coupled with other directions. In addition, it also confirms that the proposed analytical model in ETA [40] can well predict the coupling effect of biaxial loading on the shear resistance of angle bracket connections, except that when the initial load equals the peak resistance in the secondary direction, the analytical equation lower estimates the shear resistance.

Chapter 4: Conclusion

This two-part research was developed and carried out to bridge the knowledge gap in the behaviour of wall-to-floor CLT angle bracket connections under various loading scenarios. Part 1 (**2**) assesses the in- and out-of-plane performance of these connections in four directions: in-plane uplift (F1 in **Figure 2.2**), in-plane shear (F2 in **Figure 2.2**), out-of-plane tension (F3 in **Figure 2.2**), and out-of-plane compression (F4 in **Figure 2.2**). Monotonic and cyclic experimental tests were performed to evaluate the most efficient fastener type for the angle brackets connected to CLT wall and floor, and fill the research gap on the out-of-plane (perpendicular to wall plane) behaviour of angle bracket connections and the contribution of these connections in resisting out-of-plane wind and earthquake loads. The tests were carried out using two types of angle brackets, namely A90 and A105. The performance of the connections was assessed in terms of strength, stiffness, ductility, energy dissipation (only for cyclic tests), and failure modes for each loading scenario. The following conclusions are made from Part 1 tests:

- In-plane cyclic uplift and shear (Cyclic F1 and F2) tests failed largely in ductile manners due to combinations of yielding of brackets and yielding or pull-out of screws. The splitting of CLT panels was captured in few tests in large displacements. High ductility and energy-dissipation were achieved in both uplift and in-plane shear directions.
- Out-of-plane tension (F3) tests primarily failed in the splitting of CLT panels under perpendicular to grain tension load, except for A90 brackets with partially-threaded screws that exhibited ductile failures due to screw withdrawal. A105 brackets showed significantly higher strength than A90 brackets in tension. Out-of-plane compression tests, however, exhibited ductile failures. The two sizes of angle brackets achieved comparable strength, with more ductility captured in A90 samples. Since wind and seismic load can induce both out-of-plane tension and compression to angle bracket connections, these connections should be designed within their elastic range to avoid brittle failure.
- Angle brackets with fully-threaded screws exhibit higher strength and stiffness and dissipated more energy than angle brackets with partially-threaded screws in uplift, in-plane shear and out-of-plane tension tests. However, angle brackets with partially-threaded screws exhibited more ductile performance in some cases.

Part 2 (**3**) builds upon the findings of Part 1 and utilizes 3D finite element ABAQUS models to investigate the biaxial performance of CLT angle bracket connections under combinations of in- and out-of-plane loads. The numerical model was developed for one angle bracket type and verified using the monoaxial test results in Part 1. The model was then used to evaluate the biaxial performance of the angle bracket connections. The connections were loaded in two sequential steps. First, four levels of initial displacements (relative to 25%, 50%, 75% and 100 % of peak load) were applied to the connection along a secondary direction (i.e., F1: uplift, F3: tension, or F4: compression). Then, the connections were loaded up to 70 mm displacement along the shear (F2) direction in all cases. Using 3D fasteners in the model, instead of commonly-used spring-element fasteners, provided better insight into the interactions among fasteners, angle brackets and CLT panels, and failure mechanisms of angle bracket connections under biaxial loads. The performance of the connections under biaxial loads was evaluated in terms of strength, stiffness, ductility ratio, and failure modes, and compared with the shear performance of connections without initial loading. Part 2 results show that:

- The co-existence of in-plane uplift and out-of-plane tension and compression forces reduced the shear strength, stiffness, and ultimate displacement of angle bracket connections. When the initial displacement induced 25% of P_{peak}, the angle bracket connections under biaxial loads experienced similar failure modes to those under monoaxial loads (e.g. the combinations of twist and yielding of brackets, and yielding or pull out of screws). However, at higher initial load levels (i.e. 50%, 75%, and 100%), connections experienced different failure modes due to the impact of initial loads.
- The shear performance of the connections is strongly coupled with other directions. The proposed analytical model in ETA (European Technical Assessment, 2018) can well predict the coupling effect of biaxial loading on the shear resistance of angle bracket connections, except that the analytical equation provides a conservative estimate for the shear resistance when the initial load equals the peak resistance in the secondary direction.

4.1 Scope of the research

The results and conclusions of this study are limited to mentioned specimens and modelling settings (e.g. parts, processes, and techniques). Although authors expect the results to apply to other types of CLT angle bracket connections, the results may differ under other circumstances.

Future works may study the biaxial performance of other types of connections (e.g. hold-downs) and the impact of using different fastener types simultaneously (e.g. large and small screws together) on the performance of the connections.

References

[1] S. Rezvani and L. Zhou, “Numerical Modelling Analysis of Angle Bracket Connections Used in Cross Laminated Timber Constructions,” *Modul. Offsite Constr. Summit Proc.*, no. 2014, pp. 421–428, 2019, doi: 10.29173/mocs122.

[2] S. Rezvani, L. Zhou, and C. Ni, “Experimental evaluation of angle bracket connections in CLT structures under in- and out-of-plane lateral loading,” *Eng. Struct.*, vol. 244, no. October, pp. 1–20, 2021, doi: https://doi.org/10.1016/j.engstruct.2021.112787.

[3] R. Tomasi and I. Smith, “Experimental Characterization of Monotonic and Cyclic Loading Responses of CLT Panel-To-Foundation Angle Bracket Connections,” *J. Mater. Civ. Eng.*, vol. 27, no. 6, p. 04014189, 2015, doi: 10.1061/(asce)mt.1943-5533.0001144.

[4] G. D’Arenzo, G. Rinaldin, M. Fossetti, and M. Fragiacomo, “An innovative shear-tension angle bracket for Cross-Laminated Timber structures: Experimental tests and numerical modelling,” *Eng. Struct.*, vol. 197, no. June, p. 109434, 2019, doi: 10.1016/j.engstruct.2019.109434.

[5] G. D’Arenzo, R. D. Cottonaro, G. Macaluso, and M. Fossetti, “Mechanical characterization of an innovative wall-to-floor connection for Cross-Laminated Timber structures,” no. September, 2019.

[6] A. Hossain, M. Popovski, and T. Tannert, “Cross-laminated timber connections assembled with a combination of screws in withdrawal and screws in shear,” *Eng. Struct.*, vol. 168, no. April, pp. 1–11, 2018, doi: 10.1016/j.engstruct.2018.04.052.

[7] I. Gavric, “Seismic Behaviour of Cross-Laminated Timber Buildings,” 2013.

[8] M. Latour and G. Rizzano, “Cyclic behavior and modeling of a dissipative connector for cross-laminated timber panel buildings,” *J. Earthq. Eng.*, vol. 19, no. 1, pp. 137–171, 2015, doi: 10.1080/13632469.2014.948645.

[9] M. Popovski, H. G. L. Prion, and E. Karacabeyli, “Seismic performance of connections in heavy timber construction,” *Can. J. Civ. Eng.*, vol. 29, no. 3, pp. 389–399, 2002, doi: 10.1139/l02-020.

[10] M. Wang, X. Song, X. Gu, Y. Zhang, and L. Luo, “Rotational behavior of bolted beam-to-column connections with locally cross-laminated glulam,” *J. Struct. Eng.*, vol. 141, no. 4, p. 4014121, 2015.

[11] Wood First Act, “Legislative Session: 1st Session, 39th Parliament, First Reading, Bill 9-2009,” 2009.

[12] S. Rezvani, L. Zhou, and C. Ni, “Numerical analysis of in- and out-of-plane coupling effects on angle bracket connections in CLT structures,” 2021.

[13] S. Breneman, M. Timmers, and D. Richardson, “Tall Wood Buildings in the 2021 IBC: Up to 18 Stories of Mass Timber.” Woodworks Wood products council, Washington, DC, USA, 2019.

[14] International Building Code, *International building code*. International Code Council, 2021.

[15] J. Sorensen, “2020 NBCC code brings new era for Canadian wood construction,” *Journal of Commerce*, 2019. https://canada.constructconnect.com/joc/news/government/2019/05/2020-nbcc-code-brings-new-era-canadian-wood-construction.

[16] R. Brandner, G. Flatscher, A. Ringhofer, G. Schickhofer, and A. Thiel, “Cross laminated timber (CLT): overview and development,” *Eur. J. Wood Wood Prod.*, vol. 74, no. 3, pp. 331–351, 2016, doi: 10.1007/s00107-015-0999-5.

[17] L. Franco, L. Pozza, A. Saetta, M. Savoia, and D. Talledo, “Strategies for structural modelling of CLT panels under cyclic loading conditions,” *Eng. Struct.*, vol. 198, no. January, p. 109476, 2019, doi: 10.1016/j.engstruct.2019.109476.

[18] Construction Review Online, “Top 5 tallest timber buildings in the world,” 2021. https://constructionreviewonline.com/biggest-projects/top-5-tallest-timber-buildings-in-the-world/.

[19] E. Poirier, M. Moudgil, A. Fallahi, S. Staub-French, and T. Tannert, “Design and construction of a 53-meter-tall timber building at the university of British Columbia,” *Proc. WCTE*, 2016.

[20] I. Gavric, M. Fragiacomo, and A. Ceccotti, “Cyclic behavior of CLT wall systems: Experimental tests and analytical prediction models,” *J. Struct. Eng. (United States)*, vol. 141, no. 11, pp. 1–14, 2015, doi: 10.1061/(ASCE)ST.1943-541X.0001246.

[21] M. Latour and G. Rizzano, “Seismic behavior of cross-laminated timber panel buildings equipped with traditional and innovative connectors,” *Arch. Civ. Mech. Eng.*, vol. 17, no. 2, pp. 382–399, 2017, doi: 10.1016/j.acme.2016.11.008.

[22] M. Snow, A. Asiz, Z. Chen, and Y. H. Chui, “North American practices for connections in wood construction,” *Prog. Struct. Eng. Mater.*, vol. 8, no. 2, pp. 39–48, 2006.

[23] L. a. Soltis and M. Ritter, “Mechanical Connections in Wood Structures: Chapter 1--Introduction,” 1996.

[24] L. M. Ottenhaus, M. Li, and T. Smith, “Structural performance of large-scale dowelled CLT connections under monotonic and cyclic loading,” *Eng. Struct.*, vol. 176, no. April, pp. 41–48, 2018, doi: 10.1016/j.engstruct.2018.09.002.

[25] L. Pozza, A. Saetta, M. Savoia, and D. Talledo, “Angle bracket connections for CLT structures: Experimental characterization and numerical modelling,” *Constr. Build. Mater.*, vol. 191, pp. 95–113, 2018, doi: 10.1016/j.conbuildmat.2018.09.112.

[26] I. Gavric, A. Ceccotti, and M. Fragiacomo, “Experimental cyclic tests on cross-laminated timber panels and typical connections,” *Anidis*, 2011, [Online]. Available: http://scholar.google.com/scholar?hl=en&btnG=Search&q=intitle:Experimental+cyclic+tests+on+cross-laminated+timber+panels+and+typical+connections#0.

[27] I. Gavric, M. Fragiacomo, and A. Ceccotti, “Cyclic behaviour of typical metal connectors for cross-laminated (CLT) structures,” *Mater. Struct. Constr.*, vol. 48, no. 6, pp. 1841–1857, 2015, doi: 10.1617/s11527-014-0278-7.

[28] A. Jorissen and M. Fragiacomo, “General notes on ductility in timber structures,” *Eng. Struct.*, vol. 33, no. 11, pp. 2987–2997, 2011, doi: 10.1016/j.engstruct.2011.07.024.

[29] M. Izzi, A. Polastri, and M. Fragiacomo, “Investigating the Hysteretic Behavior of Cross-Laminated Timber Wall Systems due to Connections,” *J. Struct. Eng.*, vol. 144, no. 5, pp. 1–10, 2018, doi: 10.1061/(ASCE)ST.1943-541X.0002022.

[30] L. Pozza, B. Ferracuti, M. Massari, and M. Savoia, “Axial – Shear interaction on CLT hold-down connections – Experimental investigation,” *Eng. Struct.*, vol. 160, no. January 2017, pp. 95–110, 2018, doi: 10.1016/j.engstruct.2018.01.021.

[31] J. Schneider, “Conventional and novel timber steel hybrid connections: testing, performance and assessment,” 2015.

[32] CSA O86:19, “Engineering design in wood,” 2019.

[33] L. Pozza, A. Saetta, M. Savoia, and D. Talledo, “Coupled axial-shear numerical model for CLT connections,” *Constr. Build. Mater.*, vol. 150, pp. 568–582, 2017, doi: 10.1016/j.conbuildmat.2017.05.141.

[34] D. Casagrande, A. Polastri, T. Sartori, C. Loss, and M. Chiodega, “Experimental campaign for the mechanical characterization of connection systems in the seismic design of timber buildings,” 2016.

[35] G. Tamagnone, G. Rinaldin, and M. Fragiacomo, “A novel method for non-linear design of CLT wall systems,” *Eng. Struct.*, vol. 167, pp. 760–771, 2018.

[36] H. Leach, “Interstorey Drift Performance of Timber Beam-Hanger Connections,” 2018.

[37] J. Liu and F. Lam, “Experimental test of coupling effect on CLT angle bracket connections,” *Eng. Struct.*, vol. 171, no. January, pp. 862–873, 2018, doi: 10.1016/j.engstruct.2018.05.013.

[38] G. D’Arenzo, G. Rinaldin, M. Fossetti, M. Fragiacomo, F. Nebiolo, and M. Chiodega, “Tensile and shear behaviour of an innovative angle bracket for CLT structures,” *WCTE 2018 - World Conf. Timber Eng.*, 2018.

[39] G. Flatscher, G. Schickhofer, and K. Bratulic, “Experimental tests on cross- laminated timber joints and walls,” in *Proceedings of the Institution of Civil Engineers*, 2015, vol. 168.

[40] European Technical Assessment, “European Technical Approval ETA-08/0183,” 2018.

[41] C. Hughes, “Behaviour of multi-storey cross-laminated timber buildings under lateral loading,” The University of British Columbia, 2020.

[42] ASTM E2126 − 11 (Reapproved 2018), “Standard Test Methods for Cyclic (Reversed) Load Test for Shear Resistance of Vertical Elements of the Lateral Force Resisting Systems for Buildings,” 2018.

[43] ISO 16670, “Timber structures — Joints made with mechanical fasteners — Quasi-static reversed-cyclic test method,” 2003.

[44] C. Aranha, J. Branco, P. Lourenço, G. Flatscher, and G. Schickhofer, “Finite element modelling of the cyclic behaviour of CLT connectors and walls,” *WCTE 2016 - World Conf. Timber Eng.*, pp. 3501–3508, 2016.

[45] J. Liu and F. Lam, “Experimental test of coupling effect on CLT hold-down connections,” *Eng. Struct.*, vol. 178, pp. 586–602, 2019.

[46] J. Liu, F. Lam, R. O. Foschi, and M. Li, “Modeling the coupling effect of CLT connections under biaxial loading,” *J. Struct. Eng.*, vol. 146, no. 4, p. 4020040, 2020.

[47] S. R. Hollenbeck, “Numerical Modeling of Mass Timber Connections,” Oregon State University, 2018.

[48] D. E. Kretschmann, *Wood Handbook, Chapter 05: Mechanical Properties of Wood*, vol. 11W3. 2010.

[49] Z. Hashin, “Failure criteria for unidirectional fiber composites,” 1980.

[50] Z. Hashin and A. Rotem, “A fatigue failure criterion for fiber reinforced materials,” *J. Compos. Mater.*, vol. 7, no. 4, pp. 448–464, 1973.

[51] Michael Smith, “ABAQUS/Standard User’s Manual, Version 2019,” 2019.

[52] European Technical Assessment, “European Technical Approval ETA-11/0190,” 2016.

[53] ASTM D1761 − 12, “Standard Test Methods for Mechanical Fasteners in Wood,” 2012. doi: 10.1520/D1761-12.Copyright.